Response to reviewers

Dual state/rainfall correction via soil moisture assimilation for improved streamflow simulation: Evaluation of a large-scale implementation with SMAP satellite data

Yixin Mao, Wade T. Crow, Bart Nijssen

Revision summary:

We appreciate the comments from the reviewers. We respond to each reviewer comment below, with reviewer comments shown in **bold**. We have also made minor edits throughout the manuscript to make it more succinct and readable.

Response to Reviewer 1 (Christian Massari)

Major comments:

1) I have only one major comment which is related to the rainfall correction and its effect on the streamflow simulations which to me is a bit ambiguous and should be improved. In many parts of the manuscript it is said that the correction of the rainfall has a smaller effect since the rainfall forcing used (IMERG-ER) has a good quality (see lines 331 onward). However, this contradict with the results in Table 3 where the open loop simulations show in some cases of very poor performance of flood simulations (which are likely due the poor rainfall quality) and with other sentences stating that the IMERG-ER has large errors (line 448) in some basins. In fact, when forced by NLDAS2 there is a significant increase of the model performance up to 80% of PER which however, is still not satisfactory for some basins (see Table 3 Walnut, Chikaskia and Spring). Then, I think there two possible reasons. Either SMAP adds little in terms of rainfall correction or SMART only corrects for the random error component which is the component the hydrological model is less sensitive to as correctly stated by the authors. Therefore the systematic error can be very important in this respect. However as between the two precipitation products it is difficult to judge which one is really better (at least by looking at the performance in terms of KGE). I suggest to compare them with a gauge-based dataset like CPC or Stage IV both in terms of rainfall (bias, correlation and error) and in terms of streamflow simulations. Indeed it is well known that these two products works really well in US (see for example the last study of Beck et al. 2019 where they used Stage IV as a reference for validating precipitation products over CONUS). Another solution could be to drive VIC model with IMERG final run which is corrected with rain gauge and therefore should have a lower bias with its near real time counterpart and thus would explain if the systematic error is the real problem. To summarize my suggestion is to

include in the study a reference precipitation product against to compare IMERG-ER and NLDAS2. That would shed some light on the problems of the poor performance simulations.

We have responded the reviewer's comment via the following points:

1) We agree with the reviewer that we overstated the "good quality" of IMERG, since it is clear from our streamflow results that IMERG rainfall quality is not good in some sub-basins. To address this, we have toned down the argument that IMERG has "good quality", and instead emphasized that one reason of the smaller rainfall correction results than found by previous studies is because of the *relatively* better quality IMERG compared to older rainfall products (this discussion is now moved to Section 4.1 in the manuscript). In addition, the revised manuscript now clearly acknowledges (in Section 3.2.2) that in some sub-basins (the Bird, Spring, Illinois and Deep sub-basins in our experiment), SM-based rainfall correction scheme can potentially play an important role in improving VIC streamflow estimates because of relatively large IMERG error (with respect to the NLDAS-2 baseline). However, such potential improvement was not realized because these basins are densely vegetated with (subsequently) low SMAP quality. We believe that these revisions make our discussion more consistent, and balance and address the contradiction noted by the reviewer.

2) Regarding the addition of gauge-based rainfall dataset – the NLDAS-2 product used in the study is indeed already based on the gauge-based CPC rainfall (as well as ground radar), which is the reason that we used it as the reference precipitation in our study. Even if NLDAS-2 rainfall is not perfect especially when translating into streamflow results (as can be seen from our streamflow analysis), its reliance on gauge observations ensures that it is relatively more reliable than the other satellite-based rainfall products considered in this study. Therefore, it provides an adequate benchmark to evaluate the lower-quality satellite-based products. We have added a more detailed description of the NLDAS-2 rainfall product in Section 2.2.4 to highlight these points.

Response to Reviewer 2

The topic is of interest to hydrological community and the some of the conclusions made are important. However, the quality of writing not up the standard of HESS. As the authors have acknowledged that the methods used in this paper have already been implemented elsewhere in the literature, and the only "new" contribution is in terms of using new datasets, there should have been deeper discussion and analysis regarding the outcome of this experiment. I agree that authors have used Ensemble Smoother as an extension to EnKF in this work. However, the results suggest improvements only when the updates are made at coarse temporal scale (SMAP scale). So, apart from minor differences, there may not be statistically significant difference in terms of performance between the two techniques. I will be glad if I am proven otherwise. Also, most importantly, there was

only a speculative attribution of lack of improvement in performance to the better quality of IMERG precipitation. The results lack appropriate robust quantitative analysis in this regard. Further comments are listed below. In summary, the manuscript may have to be revised thoroughly in a wat that highlights the major contributions, and also show how these contributions are helping us to extend our understanding in this domain of research. In this process, please also consider addressing the following specific and minor comments:

Major comments:

1) SMAP soil moisture estimates have a maximum sensing depth up to 6 cm in vegetated areas (Babaeian et al., 2019, Reviews of Geophysics). The deeper soil moisture has stable temporal dynamics compared with that of surface soil moisture. Further, the VIC model executed at 10, 40 and 93 cm. In the process of assimilation, the SMAP soil moisture are rescaled to VIC soil moisture dynamics. So, essentially the noisier timeseries (surface soil moisture) is being rescaled using the temporal dynamics of smoother timeseries (VIC soil moisture). Can authors assess the implications of this mismatch on the final outcome?

We agree with the reviewer that matching a satellite-observed soil moisture product with that represented in a land surface model (LSM) is a very challenging task, and so far there is no standard good solution despite many research efforts (see, e.g., Yilmaz and Crow, 2013; Kumar et al., 2015; Nearing et al., 2018). On the one hand, although SMAP is typically described as measuring the top ~ 5 cm of soil moisture, the actual vertical support depth is unclear and varies nonlinearly as a function of soil moisture and vegetation water content. On the other hand, the relationship between the top-layer depth and its soil moisture dynamics in an LSM is complex and driven by a large number of poorly known model parameters (although, Shellito et al. (2018) found that changing the top-layer depth from 10 cm to 5 cm in the Noah LSM did not affect surface soil moisture dynamics much). Therefore, contrasts between the spectral characteristics of modelled and observed "surface" soil moisture is a general problem for essentially all land data assimilation systems (Qiu et al., 2014) – even those in which a concerted effort is made to "match" the vertical support of both estimates. While it likely does introduce some time scale error, the moment-matching rescaling techniques as used in our study is one of the standard, although imperfect, solutions, which is commonly used in soil moisture data assimilation studies. Therefore, we have kept our original procedure and added new discussion in Section 4.2 which acknowledges this shortcoming.

2) How is the soil moisture state in the deeper layers being updated? Is there a correction factor implemented here, as carried out by Lievens et al. (2015, 2016)? Although authors have mentioned in Line 221, an equation will bring clarity to their statement.

In our 3-layer VIC setup, the middle layer is updated using the surface measurement via a standard EnKF algorithm (i.e., perturbed and updated based on the error covariance calculated based on the ensemble distribution) – this follows the approach of Lievens et al. (2016) but differs slightly from Lievens et al. (2015) where an artificial vertical correlation factor was used to “nudge” the deeper-layer state. For the bottom layer, we did not include it in the EnKF update, which is the same as in Lievens et al. (2015, 2016) and further justified by Mao et al. (2019). We still perturbed the bottom layer to create a realistic ensemble estimate. All these modeling choices were detailed earlier in Mao et al. (2019), and now clarified in the revised text (and with additional equations in Supplemental material).

3) Equations will help to understand the mathematically involved procedure like data assimilation.

We have added the key equations and descriptions in Supplemental Material as suggested.

4) Authors may have to discuss the sensitivity of choosing gamma parameter in Eq. (1).

First, we would like to emphasize that the gamma parameter in Equation (1) was already manually tuned with the objective of maximizing the correlation coefficient between the uncorrected API time series and the SMAP time series over the domain, such that the API model as stated in Equation (1) captures the SMAP-observed SM dynamics as much as possible. In addition, this issue has been examined in past studies. Using a very similar system, Crow et al. (2011) found that the magnitude of rainfall correction was minimally sensitive to variations in gamma in the effort of mimicking a more complex soil water balance model.

Second, we have added a sensitivity analysis to examine the impact of gamma on rainfall correction results, as suggested by the reviewer. Figures 1 and 2 below show the domain-median correlation coefficient improvement and percent RMSE reduction (PER), respectively, after correction at different gamma values (in the manuscript, gamma = 0.98 was used). We see that around the chosen gamma = 0.98, the sensitivity of rainfall correction performance to gamma is relatively small, and gamma = 0.98 results in optimal PER when evaluating at 1-day and 3-day time steps (although performance is even better at gamma = 0.99 for the other measures shown). However, we also see that the correction performance is significantly degraded if gamma is far from the chosen value (i.e., if gamma < 0.95). These results should confirm that the chosen gamma value in the manuscript is reasonable and roughly optimal. This analysis is now presented in the revised Supplemental Material.

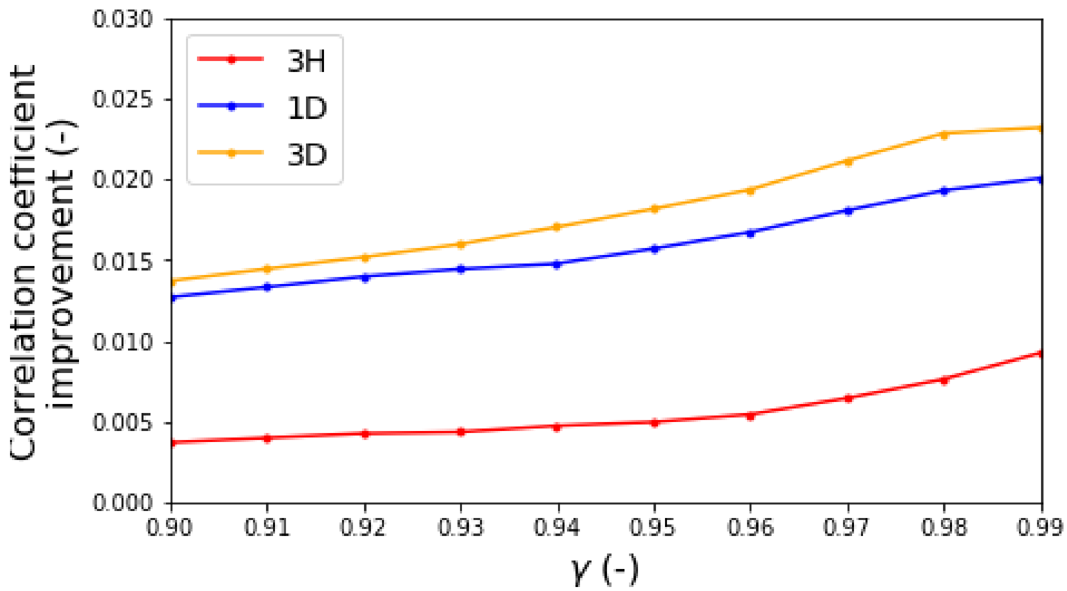

Figure 1. Domain-median correlation coefficient improvement of IMERG rainfall after SMART correction (with respect to the NLDAS-2 reference) at different γ values. The improvement is evaluated for 3-hour (3H), 1-day (1D) and 3-day (3D) accumulation intervals.

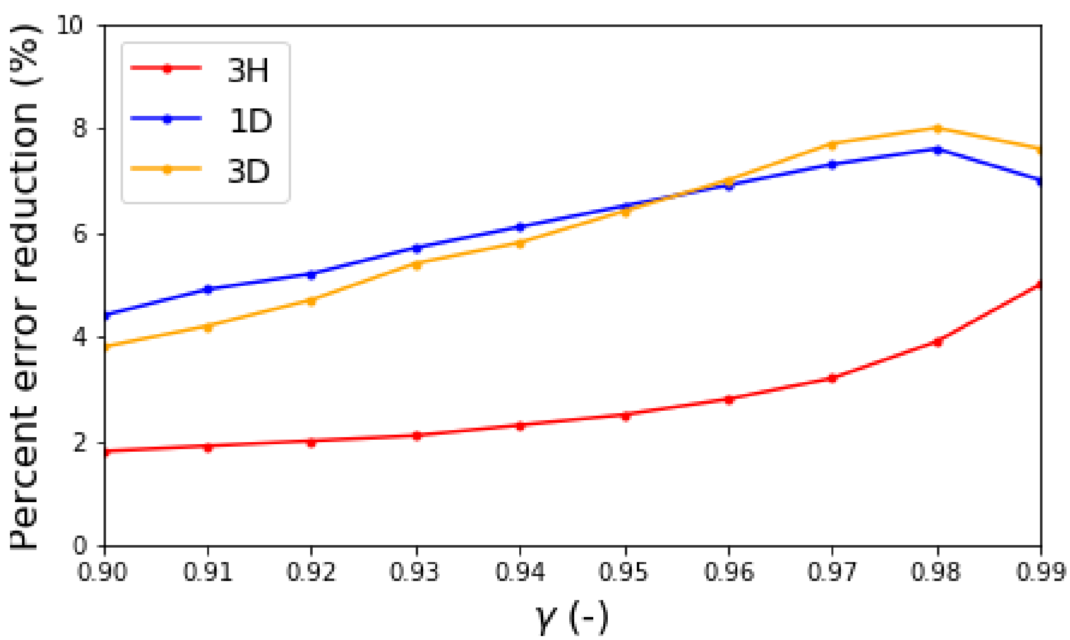

Figure 2. Same as Figure 1, but evaluated by percent RMSE reduction (PER).

5) L 210: There is also a need for authors to explain why the error variance of 0.3 mm2 is chosen and its sensitivity.

According to the Kalman filter theory, the time series of the normalized filter innovation should have mean zero and variance one. The normalized filter innovation, *e*, is defined as

$$e_k = \frac{\tilde{y}_k - \tilde{y}_k^-}{\sqrt{H_k P_k^- H_k^T + R_k}} \quad (1)$$

where k is the time step index, $\tilde{y}$ is the measurement, $\tilde{y}^-$ is the estimated measurement before update, H is the vector mapping from state to measurement space, P^- is the estimated state error covariance, and R is the measurement error variance. Since we have a relatively good estimate of measurement error, the only degree of freedom to tune the innovation variance is the state error level, for which 0.3 mm^2 was found to roughly satisfy the statistical requirement on the filter innovation. Since the innovation is required to have these statistical properties by the Kalman filter theory, this is not something that can be freely altered and we did not carry out a sensitivity analysis. This point has been clarified in the revised text.

6) L: 228: When only top two layers are being updated, why is it that all the three layers are perturbed?

While the perturbation of the bottom layer does not affect the EnKF updating procedure, we need to perturb the bottom layer to generate a realistic ensemble for it since we are interested in probabilistic streamflow estimation (and the bottom layer soil moisture impacts VIC streamflow estimates via its role in determining baseflow). While ensemble spread in the first two soil layers will eventually propagate into the (third) bottom layer, such spread does not explicitly account for errors that originate in the bottom layer. We have clarified it in the text.

7) L: 230-233: I find that this statement in qualitative in nature. So, it cannot be considered as a finding.

We did carry out the experiment of comparing the state update performance with and without considering the spatial auto-correlation of states, and found that considering spatial autocorrelation did not improve EnKF result (detailed results not shown). We have clarified this in the revised text.

8) Figure 3 is not explained properly. What is the meaning of improvement in correlation? Is it correlation (NLDAS, IMERG_Corrected) – correlation(NLDAS, IMERG_Original)? There is no detail about it in the manuscript.

Figure 3 shows the improvement of the IMERG rainfall product relative to the NLDAS-2 reference before and after the SMART rainfall correction - the formula written out by the reviewer is correct. However, we have decided to leave out this formula to avoid extra notation, but instead added a clearer description in the caption.

9) L: 302: If delta and P are aggregated to 3-day windows prior to correction in the case of EnKF, why are there minor changes in the spatial maps in Fig. 3 (d-f)? Will it not be sensible to just have a 3-day window map?

Even if EnKF corrects the 3-day accumulated rainfall amounts, the 3-day rainfall delta is downscaled uniformly to every 3-hour time step under the 3-day window. Therefore, the 3-hourly (or daily) rainfall can still be improved to be closer to truth, even if the correction does not capture the fine temporal resolution. We have clarified this in the revised text.

10) Interestingly, there seems to be an overlap in the spatial patterns of Figs. 2 and 3. It appears that there is a correlation improvement in the western part, which received lower rainfall compared to the eastern region. Is there such dependence of rainfall amount on the performance of correction?

We have added discussion on the spatial pattern of rainfall correction as suggested by the reviewer (first paragraph of Section 3.1.2). Specifically, SMAP tends to have better quality (in terms of correlation improvement) in the western part of the domain due to less vegetation, which is one possible reason that it adds more value to the SMART rainfall correction in the western region. RMSE is reduced more in the eastern part of the domain, which is likely due to the better correction for larger rainfall events (which mostly happen in the east).

11) I think it will be better if bias and error maps are also plotted to comprehensively characterize the errors.

The error (in terms of RMSE) reduction map was already included in the manuscript (Figure 5, left column). We do not include a bias correction map since the SMART algorithm does not correct overall rainfall bias – it rescales the corrected time series back to have the same mean as the uncorrected time series (this is pointed out in the first paragraph of Section 3.1.1).

12) L: 333-334: This is one of the most important statements made by authors. I think it is important to support this statement with rigorous analysis. I think it may not be fair to compare these results with that of Table 2. This is because of a) the experimental setup has changed, b) case study has changed, and c) the reference dataset has changed.

First, we have toned down the argument that IMERG has "good quality", and instead emphasized the main reason for the smaller rainfall correction results than those found by previous studies is the *relatively* better quality IMERG compared to older rainfall products. We have also pointed out that SMAP's quality is low in dense-biomass regions, which limits its ability to correct IMERG rainfall. Therefore, the revised manuscript now relies less heavily on this argument to explain key results.

Nevertheless, the tendency for marginal data assimilation improvement to decrease as the skill of the background increases is a very well-developed *general* concept in land data assimilation (Reichle et al., 2008; Qing et al., 2011; Bolten and Crow, 2012; Dong et al., 2019) – and has already been demonstrated for the specific case of using soil moisture to correct rainfall (Crow et al., 2011). In addition, Crow and Ryu (2009) already provided exactly the rigorous analysis requested by the author. That is, using a conceptually equivalent rainfall correction approach and a set of well-controlled synthetic experiments, they examined the impact of baseline precipitation analysis on marginal precipitation skill improvements. Their conclusions (also) clearly demonstrate that rainfall correction margins are degraded by improvements in baseline precipitation skill (i.e., the exact point made here). Finally, while the approaches applied in Table 2 differ slightly, it should be noted that various correction approaches (e.g. the SM2RAIN used by Brocca et al. (2013, 2014) and the SMART approach applied by Crow et al. (2011)) have been inter-compared and found to perform similarly (Brocca et al., 2016), suggesting that their results are fairly cross-comparable (as in Table 2). Therefore, our hypothesis here is supported by a range of earlier studies and a well-demonstrated concept in land data assimilation. We have clarified these points in Section 4.1 in the revised manuscript.

13) Figure 3: Since there is a median correlation improvement difference of only 0.01, can't we just use EnKF, which is much simpler compared to Ensemble Smoother?

First of all, the EnKS is not really more complicated or computationally demanding than the EnKF. As a result, there is no significant downside to use the EnKS instead of an EnKF. Secondly, since the baseline correlation coefficent of IMERG is already quite good (domain-median correlation coefficient above 0.8 relative to NLDAS-2 reference), it is a relatively difficult task to further improve it, and even small correlation improvements are significant (in the context of remaining unexplained variability). Finally, the correlation improvement achieved by EnKS is also much more obvious in certain parts of the domain (e.g., western end; see Figure 3) compared to that by EnKF, despite the relatively small difference in domain-median improvement.

14) Figure 4: It is understandable that in the case of correcting rainfall at all timesteps, SMART can misinterpret SM retrieval noise as small rainfall corrections. Can this issue be alleviated by considering a threshold of, say 2 mm to classify rain/no-rain and continuously correct the rainfall. This way the SM retrieval noise can still be pushed to zero, and there may some reduction of uncertainty due to rain/no-rain classification.

We have added a sensitivity analysis as suggested by the reviewer. Specifically, we alter the threshold of classifying IMERGE rain/no rain (this threshold is essentially set to zero in the original manuscript, and SMART only corrects time steps during which rainfall occurs), and observe its impact on the rainfall correction results (i.e., categorical metrics at different rainfall scales as well as correlation improvement and percent RMSE reduction (PER)).

The following figures show the SMART correction results with different rain/no rain thresholds. For categorical metrics (Figure 1), having a rain/no rain threshold of 1 mm/3 hours or 2 mm/3 hours mitigates the issue of worsened POD at small rainfall events comparing to zero threshold, but also removes the (although small) FAR improvement. For mid-ranged rainfall events, a positive threshold mitigates the issue of worsened FAR as in the zero threshold case, but POD improvement becomes smaller. For larger rainfall events, POD improvement and TS improvement become slightly smaller (i.e., closer to zero) when using a positive rain/no rain threshold (note that the small positive rain/no rain threshold value can be considered as a "larger" rainfall event at some pixels with overall low precipitation, therefore affecting the categorical metrics toward the right side on the categorical metrics plots).

In addition to the categorical metrics, setting the rain/no rain threshold to either 1 mm/3 or 2 mm/3 hours slightly lowers values of correlation coefficient improvement and PER versus the baseline case of applying a rain/no rain threshold of zero accumulation (Figures 2 and 3).

In summary, there is no obvious optimized number for the rain/no rain threshold since there is a trade-off between POD and FAR. Although the overall TS at smaller rainfall events improves with a positive threshold, the correction for larger events, which are what SMART correction is more useful for, slightly worsens. A positive rain/no rain threshold does not benefit correlation coefficient and PER (which are sensitive to both POD and FAR performance). Based on these analyses, we have decided to keep the original analysis in the manuscript to have a zero rain/no rain threshold for SMART correction. We have added this sensitivity analysis to the revised Supplemental Material (and briefly mentioned key results of the analysis in the revised main text).

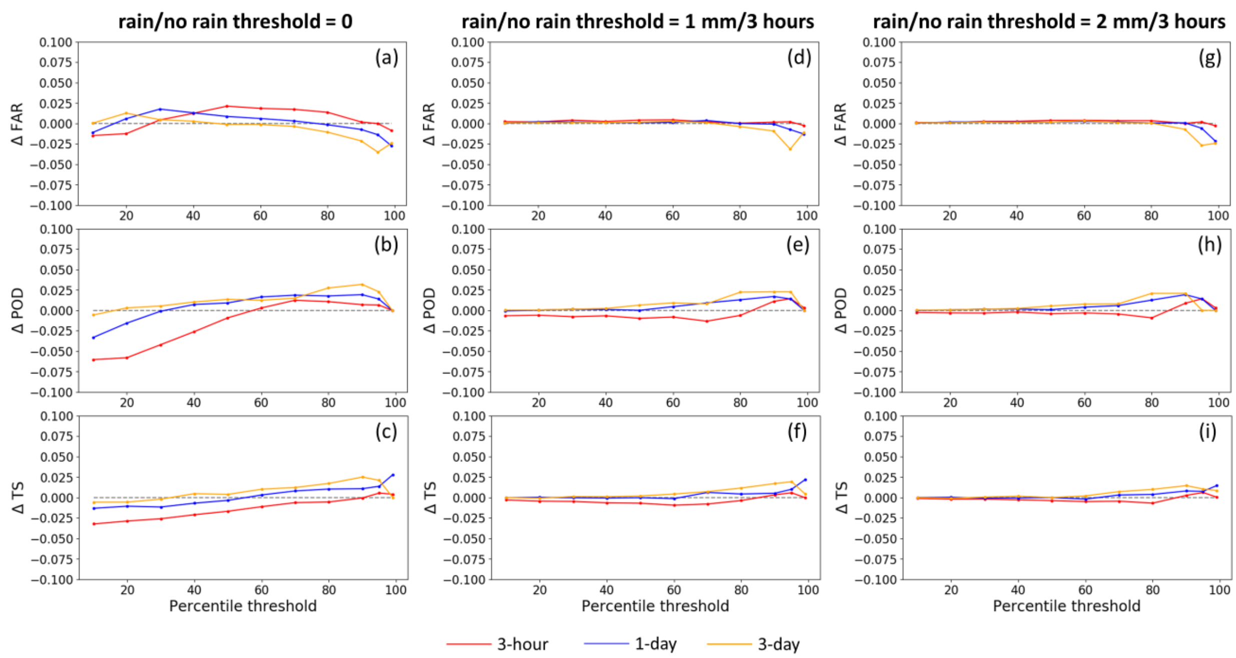

Figure 3: Change in categorical metrics (FAR, POD and TS) before and after SMART correction for 3-hourly, 1-day and 3-day accumulation periods. The left column (panels a, b and c) is the same as in Fig. 4 (right column) in the main text with SMART only correcting IMERG rainfall events with non-zero accumulation. The middle and right columns show the same metrics with SMART only correcting IMERG rainfall for events where accumulation rates exceed thresholds of 1 mm/3 hours and 2 mm/3 hours, respectively.

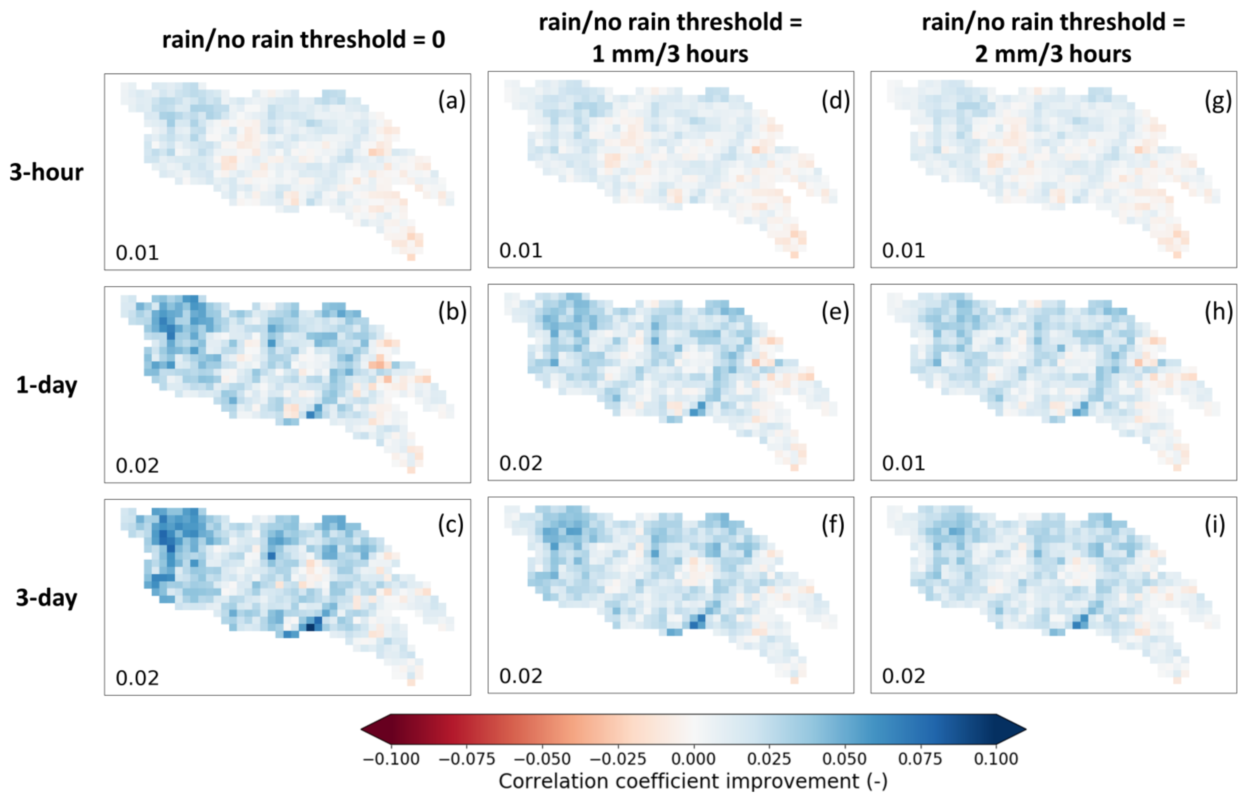

Figure 4: Correlation coefficient (with respect to the NLDAS-2 reference precipitation) improvement before and after SMART correlation for 3-hourly, 1-day and 3-day accumulation periods. As in Fig. 7, the left column (panels a, b and c) is the same as in Fig. 4 (right column) in the main text with SMART only correcting IMERG rainfall events with non-zero accumulation. The middle and right columns show the same metrics with SMART only correcting IMERG rainfall for events where accumulation rates exceed thresholds of 1 mm/3 hours and 2 mm/3 hours, respectively.

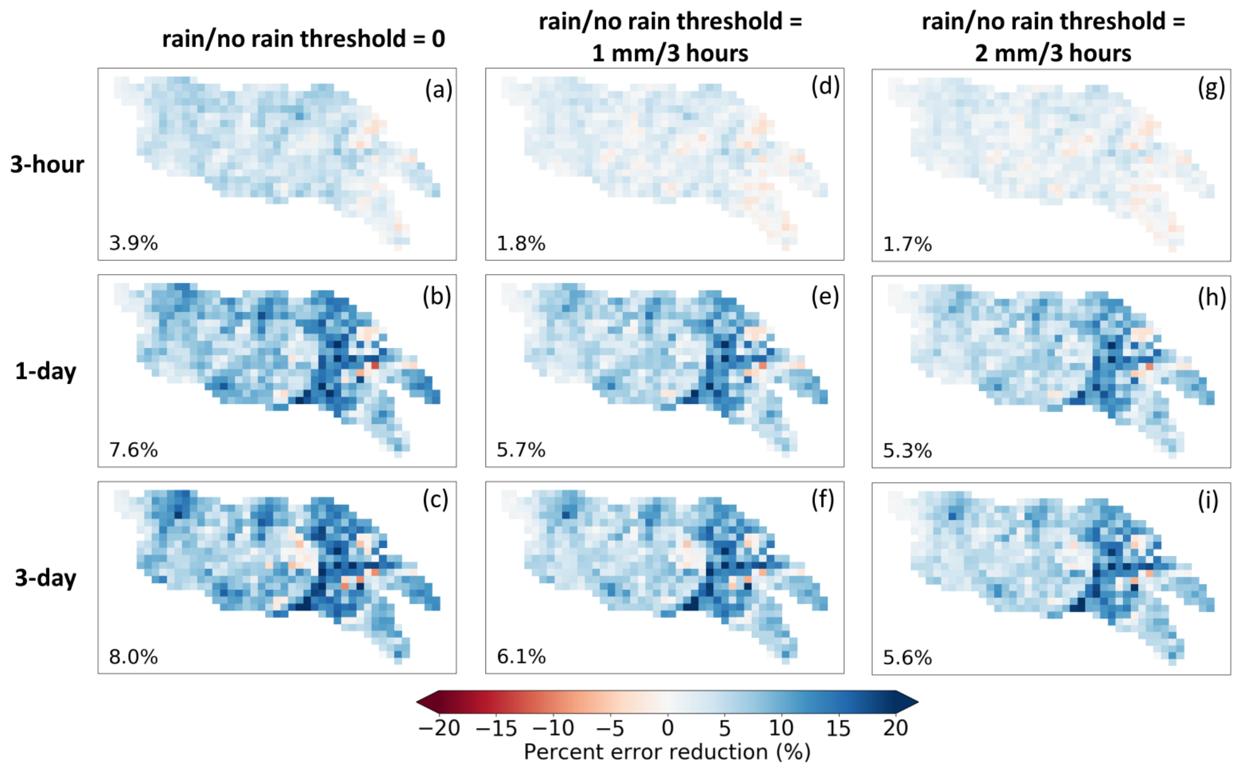

Figure 5: Same as Figure 4 above, but for percent RMSE reduction (PER; with respect to the NLDAS-2 reference precipitation). The left column (panels a, b and c) is the same as in Fig. 5 (left column) in the main text

15) L: 318 is a speculative statement with no strong analysis.

We have reworded the statement to list the improved rain/no rain detection of IMERG as one possible reason for the success of our tactic.

16) Section 3.1.2: (in alignment with my Comment 12) I think correlation may not be sufficient to conclude on the quality of rainfall product. There can be other forms of error (such as bias), which are not being considered in this analysis.

As mentioned above in Response to Reviewer 2 Major Comment 11, the original manuscript did include both an RMSE analysis (Figure 5, left column) as well as results based on a range of categorical metrics (e.g., POD, FAR and TS – see Figure 4) in the manuscript, with discussion in Section 3.1.2. We have added discussion of their spatial pattern in the revised test.

Overall bias is not designed to be corrected by the SMART algorithm and can therefore not be used as a metric for improvement (we have clarified this in Section 3.1.2).

17) Authors should provide some insights into the spatial patterns in Fig. 5. If median value is all that is needed in the discussion, then what is the need to have such spatial maps?

We have added discussion of the spatial pattern of the rainfall correction as suggested by the reviewer in Section 3.1.2. Specifically, RMSE is reduced more in the eastern part of the domain, which is likely due to the better correction for larger rainfall events (which mostly happens in the east). NENSK maps show that ensemble rainfall tends to be under-dispersed on the west edge of the domain with low rainfall, indicating that we are underestimating rainfall uncertainty in this region.

18) Section 3.2.1: I think there is a need to compare the rainfall products with a third product to get a complete picture of relative errors between the products.

As mentioned above in Response to Reviewer 1 Major Comments, NLDAS-2 precipitation is derived from daily gauge-based rainfall measurements and hourly ground-radar data, and is widely used. As a result, it is expected to be as generally reliable as any other ground-based rainfall product available in the region. Even if NLDAS-2 rainfall is not perfect (as can be seen from our streamflow results), its reliance on gauge observations ensures that it is relatively more reliable than the IMERG (and SMART-corrected) rainfall products considered in this study. Therefore, it provides an adequate benchmark for relative variation in skill and accuracy for these lower-quality products (we have added clarification on these in Section 2.2.4). We do not see any advantages of including an additional product for validation, particularly since that product will (inevitably) not be independent from NLDAS-2 (due to a shared dependence on common rain gauge datasets).

19) There is no discussion regarding Figs. 6 and 7 in the manuscript.

Figures 6 and 7 were discussed in Section 3.2.3 (the impact of VIC parameterization)..

20) Fig. 7 Deep Site: Between June and July although there are spikes in the ensemble, why isn't there a peak in dual corrected time series (which is ensemble-mean)? Also, since these are unregulated catchments, any peak can be attributed to rainfall event. So, if there are spikes in the ensemble during this period, does it mean a) there is an anomalous rainfall or b) the assimilation technique erroneously updated the rainfall during this period? I think these streamflow timeseries should also contain rainfall timeseries to look at where the update is being carried out.

As suggested by the reviewer, we have added rainfall data to the streamflow time series plot (the uncorrected IMERG rainfall (i.e., Figure 6) as well as the SMART-corrected rainfall ensemble (i.e., Figure 7). With the help of these (newly plotted) rainfall time series, the ensemble spikes at the Deep site between June and July (as an example) can be explained as follows:

1) For the spike around early July 2017: IMERG detected a small rainfall event, which correctly corresponded to a small rise in the gauge-observed streamflow. The ensemble of SMART-corrected rainfall is spread around the original IMERG time series without extreme peaks, but there are a few dual-corrected streamflow ensemble members with much-higher-than-observed spikes. This is likely because, given the hydrologic conditions during that time, 1) streamflow has a highly non-linear response to rainfall input in the VIC model, and/or 2) streamflow has a highly non-linear response to the SM state update in the VIC model.

2) For the spike around mid-June: the gauge-observed streamflow showed almost no spike at all while the uncorrected IMERG showed a small rainfall event, which indicates that this may be a false alarm event detected by IMERG. In this case, the few high-flow outlier ensemble members in the dual-corrected streamflow are likely due to both an inaccurate IMERG detection that is not successfully corrected by SMART, and the highly nonlinear response of streamflow to rainfall/SM state.

3) Because of the sometimes highly non-linear response of simulated streamflow to rainfall/state update, we plotted ensemble-median instead of ensemble-mean of the streamflow time series since the ensemble-median is a more stable representation of the "average" behavior of the streamflow ensemble. The ensemble-mean would, as the reviewer pointed out, bias toward a few outliers.

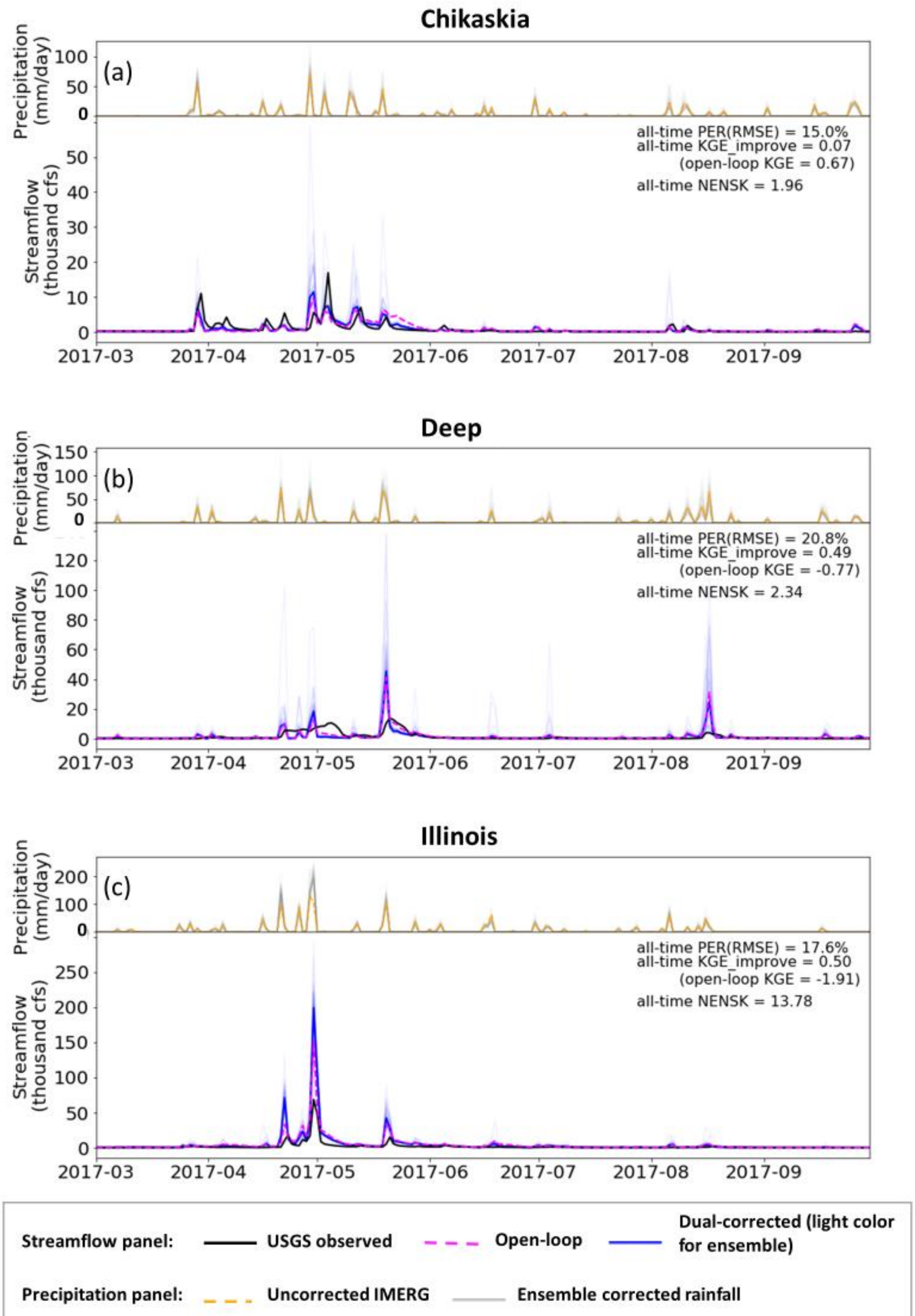
Chikaskia
(a)
Precipitation (mm/day)
Streamflow (thousand cfs)
all-time PER(RMSE) = 15.0%
all-time KGE_improve = 0.07
(open-loop KGE = 0.67)
all-time NENSK = 1.96
Deep
(b)
all-time PER(RMSE) = 20.8%
all-time KGE_improve = 0.49
(open-loop KGE = -0.77)
all-time NENSK = 2.34
Illinois
(c)
all-time PER(RMSE) = 17.6%
all-time KGE_improve = 0.50
(open-loop KGE = -1.91)
all-time NENSK = 13.78
2017-03 2017-04 2017-05 2017-06 2017-07 2017-08 2017-09
Streamflow panel:
USGS observed
Open-loop
Dual-corrected (light color for ensemble)
Precipitation panel:
Uncorrected IMERG
Ensemble corrected rainfall

Updated Figure 6. Example time series of streamflow results from the dual correction system. In the lower panel, b*lack line*: USGS observed streamflow; *magenta line*: baseline VIC simulation; *light blue lines*: ensemble updated streamflow results; *solid blue line*: ensemble-mean updated streamflow. In the upper panel, *orange line*: uncorrected IMERG rainfall aggregated to the sub-basin-average; *light grey lines*: ensemble corrected rainfall. Only part of the simulation period is shown for clear display; however, statistics shown on each panel are based on the entire simulation period (approximately 2.5 years).

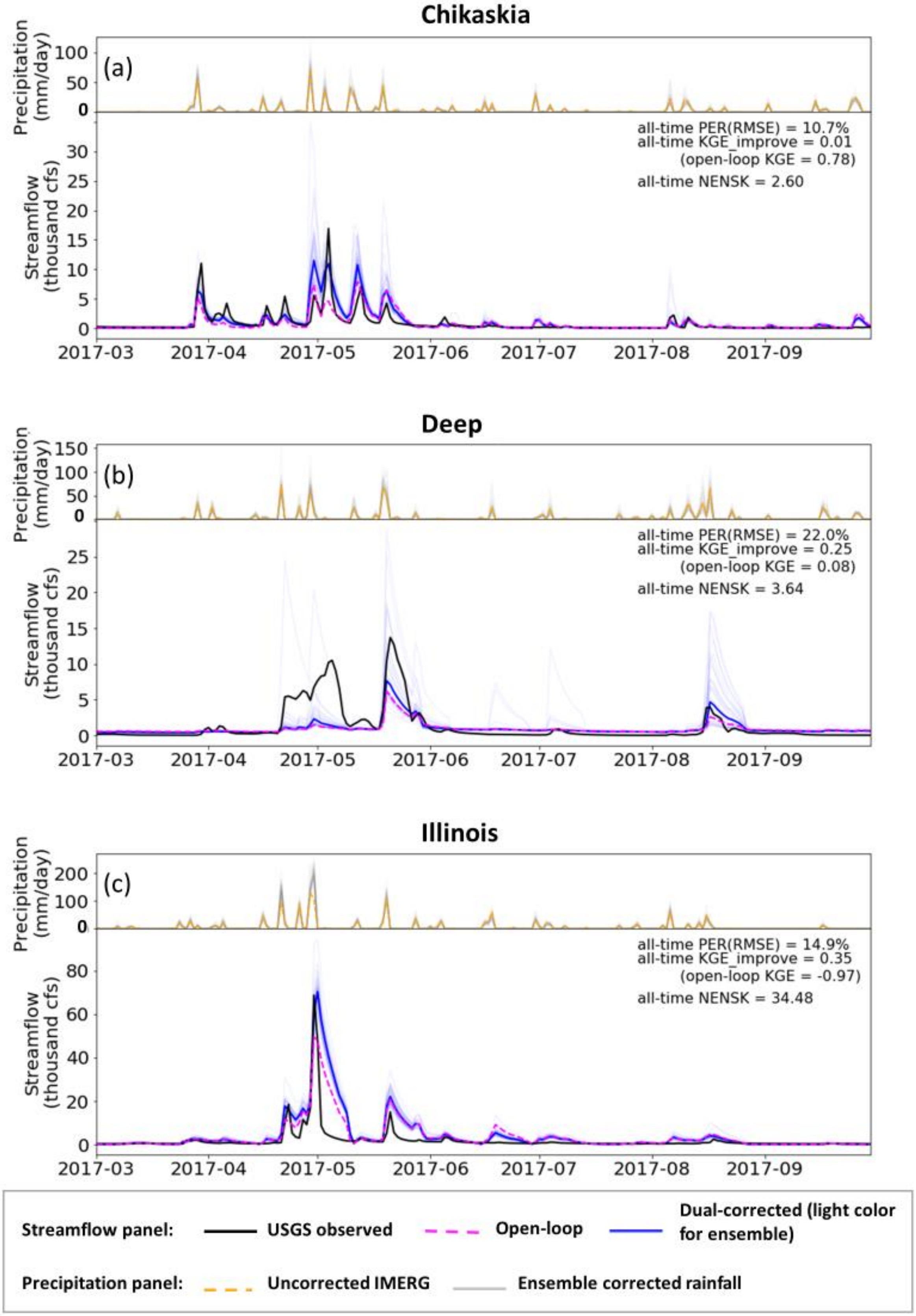

Chikaskia
(a)
Precipitation (mm/day)
Streamflow (thousand cfs)
all-time PER(RMSE) = 10.7%
all-time KGE_improve = 0.01
(open-loop KGE = 0.78)
all-time NENSK = 2.60
Deep
(b)
all-time PER(RMSE) = 22.0%
all-time KGE_improve = 0.25
(open-loop KGE = 0.08)
all-time NENSK = 3.64
Illinois
(c)
all-time PER(RMSE) = 14.9%
all-time KGE_improve = 0.35
(open-loop KGE = -0.97)
all-time NENSK = 34.48
2017-03
2017-04
2017-05
2017-06
2017-07
2017-08
2017-09
Streamflow panel:
USGS observed
Open-loop
Dual-corrected (light color for ensemble)
Precipitation panel:
Uncorrected IMERG
Ensemble corrected rainfall

Updated Figure 7. Same as Figure 6, but calibrated VIC model parameters.

21) The discussion section is speculative not very convincing. Authors may have to carry out robust analysis to substantiate their findings.

We have re-organized our results and discussion sections to incorporate all the major comments from reviewers and streamlined our major findings. Specifically:

1) We have toned down the argument that IMERG has “good quality”, and instead emphasized that the main reason for the smaller rainfall correction results than those found by previous studies is the *relatively* better quality IMERG compared to older rainfall products.

2) In addition, we pointed out that SMAP’s quality is low in dense-biomass regions, resulting in underperformed SMART rainfall correction in such regions.

3) We have emphasized our finding that systematic error accounts for a significant fraction of the total streamflow error, and the systematic error cannot be corrected by Kalman-filter-based data assimilation techniques which aimed solely at reducing zero-mean random errors.

Minor Comments:

22) Figure 4: the x-axis is not explained properly.

We have added more description of the x-axis in the figure caption.

23) Abstract opens with statement that soil moisture is necessary for accurate streamflow simulations. However, the conclusions are slightly contradictory. Please consider revising the abstract appropriately.

We have reworded the first few sentences in the abstract. We also would like to point out that soil moisture probably still contains information to help simulate streamflow more accurately, but the findings of this study show that our current satellite measurement and data assimilation techniques are not fully extracting this information.

References:

Bolten, J. D. and Crow, W. T.: Improved prediction of quasi-global vegetation conditions using remotely-sensed surface soil moisture. Geophys. Res. Lett.. 39, L19406, doi:10.1029/2012GL053470, 2012.

Brocca, L., Moramarco, T., Melone, F., and Wagner, W.: A new method for rainfall estimation through soil moisture observations, Geophys. Res. Lett., 40, 853–858, doi:10.1002/grl.50173, 2013.

Brocca, L., Ciabatta, L., Massari, C., Moramarco, T., Hahn, S., Hasenauer, S., Kidd, R., Dorigo, W., Wagner, W., and Levizzani, V.: Soil as a natural rain gauge: Estimating global rainfall from satellite soil moisture data, J. Geophys. Res. Atmos., 119, 5128–5141, doi:10.1002/2014JD021489, 2014.

Brocca, L., Pellarin, T., Crow, W. T., Ciabatta, L., Massari, C., Ryu, D., Su, C.-H., Rüdiger, C., and Kerr, Y.: Rainfall estimation by inverting SMOS soil moisture estimates: A comparison of different methods over Australia, J. Geophys. Res. Atmos., 121, 12,062–12,079, doi:10.1002/2016JD025382, 2016.

Crow, W. T., and Ryu, D.: A new data assimilation approach for improving runoff prediction using remotely-sensed soil moisture retrievals, Hydrol. Earth Syst. Sci., 12(1-16), doi:10.5194/hess-13-1-2009, 2009.

Crow, W. T., van den Berg, M. J., Huffman, G. J., and Pellarin, T.: Correcting rainfall using satellite-based surface soil moisture retrievals: The Soil Moisture Analysis Rainfall Tool (SMART), Water Resour. Res., 47, W08521, doi:10.1029/ 2011WR010576, 2011.

Dong, J., Crow, W. T., Reichle, R., Liu, Q., Lei, F. and Cosh, M.: A global assessment of added value in the SMAP Level 4 soil moisture product relative to its baseline land surface model. Geophys. Res. Lett., 46:6604-6613, doi:10.1029/2019GL083398, 2019.

Kumar, S. V., Peters-Lidard, C. D., Santanello, J. A., Reichle, R. H., Draper, C. S., Koster, R. D., Nearing, G., and Jasinski, M. F.: Evaluating the utility of satellite soil moisture retrievals over irrigated areas and the ability of land data assimilation methods to correct for unmodeled processes, Hydrol. Earth Syst. Sci., 19, 4463–4478, doi:10.5194/hess-19-4463-2015, 2015.

Lievens, H., et al.: SMOS soil moisture assimilation for improved hydrologic simulation in the Murray Darling Basin, Australia, Remote Sens. Environ., 168, 146-162, doi:10.1016/j.rse.2015.06.025, 2015.

Lievens, H., De Lannoy, G. J. M., Al Bitar, A., Drusch, M., Dumedah, G., Hendricks Franssen, H.-J., Kerr, Y. H., Tomer, S. K., Martens, B., Merlin, O., Pan, M., Roundy, J. K., Vereecken, H., and Walker, J. P.: Assimilation of SMOS soil moisture and brightness temperature products into a land surface model, Remote Sens. Environ., 180, 292-304, doi:10.1016/j.rse.2015.10.033, 2016.

Mao Y., Crow, W. T., and Nijssen, B.: A framework for diagnosing factors degrading the streamflow performance of a soil moisture data assimilation system, J. Hydrometeorol., 20(1), 79-97, doi:10.1175/JHM-D-18-0115.1, 2019.

Nearing, G., Yatheendradas, S., Crow, W.T., Chen, F. and Zhan, X: The efficiency of data assimilation, Water Resour. Res., 54:6374–6392, doi:10.1029/2017WR020991, 2018.

Qing, L., Reichle, R., Bindlish, R., Cosh, M. H., Crow, W.T., de Jeu, R., de Lannoy, G., Huffman, G. J. and Jackson, T. J.: The contributions of precipitation and soil moisture observations to the skill of soil moisture estimates in a land data assimilation system, J. Hydrometeorol.. 12(5):750-765, doi:10.1175/JHM-D-10-05000.1, 2011.

Qiu, J., Crow, W.T., Mo, X. and Liu, S: Impact of temporal autocorrelation mismatch on the assimilation of satellite-derived surface soil moisture retrievals, IEEE J-STARS, 7(8):3534-3542, doi:10.1109/JSTARS.2014.2349354, 2014.

Reichle, R. H., Crow, W. T., Koster, R. D., Sharif, H. and Mahanama, S.: Contribution of soil moisture retrievals to land data assimilation products, Geophys. Res. Lett., 35, L01404, doi:10.1029/2007GL031986, 2008.

Shellito, P. J., Small, E. E., and Livneh B.: Controls on surface soil drying rates observed by SMAP and simulated by the Noah land surface model, Hydrol. Earth Syst. Sci., 22, 1649-1663, doi:10.5194/hess-22-1649-2018, 2018.

Yilmaz, M.T. and Crow, W.T: The optimality of potential rescaling approaches in land data assimilation, J. Hydrometeorol., 14:650-660, doi:10.1175/JHMD12052.1, 2013.

Dual state/rainfall correction via soil moisture assimilation for improved streamflow simulation: Evaluation of a large-scale implementation with SMAP satellite data

Yixin Mao[1], Wade T. Crow[2] and Bart Nijssen[1]

1: Department of Civil and Environmental Engineering, University of Washington, Seattle, WA

2: Hydrology and Remote Sensing Laboratory, Agricultural Research Service, USDA, Beltsville, MD

Corresponding author: Bart Nijssen (nijssen@uw.edu)

Style Definition: Comment Text

Abstract

Soil moisture (SM) measurements contain information about both pre-storm hydrologic states and within-storm rainfall estimates, both of which are ~~essential~~required inputs for ~~accurate~~event-based streamflow ~~simulation~~simulations. In this study, an existing dual state/rainfall correction system is extended and implemented in ~~a large~~the 605,000 km^2 Arkansas-Red River basin with a semi-distributed land surface model. The ~~latest~~ Soil Moisture Active Passive (SMAP) satellite surface SM retrievals are assimilated to simultaneously correct antecedent SM states in the model and rainfall estimates from the ~~latest~~ Global Precipitation Measurement (GPM) mission. While the GPM rainfall is corrected slightly to moderately, especially for larger events, the correction is smaller than that reported in past studies ~~because of~~due primarily to the improved baseline quality of the new GPM satellite product. ~~The~~In addition, rainfall correction is poorer in regions with dense biomass due to lower SMAP quality. Nevertheless, SMAP-based dual state/rainfall correction is shown to generally improve streamflow ~~is corrected slightly to moderately via dual correction~~ estimates, as shown by comparisons with streamflow observations across ~~8~~eight Arkansas-Red River sub-basins. ~~The correction is larger at sub-basins with poorer GPM rainfall and poorer open-loop streamflow simulations. Overall, although the dual data assimilation scheme~~ However, more substantial streamflow correction is ~~able to nudge streamflow simulations in the correct direction, it corrects only a relatively small portion of the total~~limited by significant systematic errors present in model-based streamflow ~~error. Systematic modeling error accounts for a larger portion of the overall streamflow error, which is~~estimates that are uncorrectable ~~by~~via standard data assimilation techniques~~.~~ aimed solely at zero-mean random errors. These findings suggest that ~~we may be reaching a point of diminishing returns for applying data assimilation approaches to correct random errors in streamflow simulations. More~~more substantial streamflow correction ~~would rely on~~will likely require better quality SM observations as well as future research efforts aimed at reducing ~~the~~ systematic ~~error and developing higher-quality satellite rainfall products~~errors in hydrologic systems.

1. Introduction

Accurate streamflow simulation is important for water resources management applications such as flood control and drought monitoring. Reliable streamflow simulation requires accurate estimates of pre-storm soil moisture (SM) ~~conditions~~ that control the partitioning of infiltration and surface runoff during rainfall events, as well as longer-memory subsurface flow (Freeze and Harlan, 1969; Western et al., 2002; Aubert et al., 2003). Good streamflow simulations also require realistic rainfall time series estimates.

SM measurements~~, if available,~~ contain information about both antecedent hydrologic states and ~~preceding~~within-storm rainfall events. With advances in the ~~advance~~quality and availability of in-situ and satellite-measured SM products, researchers have started to explore the potential of using SM measurements to improve the estimates of both ~~aspects.~~pre-storm SM and within-storm rainfall. For example, ~~a number of~~multiple studies have attempted to assimilate SM measurements to improve the representation of antecedent SM states in hydrologic models via Kalman-filter-based techniques (e.g., Francois et al., 2003; Brocca et al., 2010, 2012; Wanders et al., 2014; Alvarez-Garreton et al., 2014; Lievens et al., 2015, 2016; Massari et al., 2015; Mao et al., 2019). Other studies have explored ~~approaches to using~~the use of SM measurements to back-calculate within-storm rainfall or to correct existing rainfall time series products (e.g., Crow et al., 2011; Chen et al., 2012; Brocca et al., 2013; Brocca et al., 2014; Brocca et al., 2016; Koster et al., 2016).

In the ~~recent~~past decade, so-called dual state/rainfall correction systems have been implemented that combine *both* ~~the~~SM state~~-~~update and rainfall correction schemes to optimally improve streamflow simulations (e.g., Crow and Ryu, 2009; Chen et al., 2014; Alvarez-Garreton et al., 2016). Specifically, SM measurements (typically from satellite observation) are used to simultaneously update model states and correct ~~a rainfall product (also~~ the (typically satellite-observed~~).~~) rainfall time series product used to force the model. The updated antecedent states and corrected rainfall are then combined as inputs into a hydrologic model to produce an improved streamflow simulation (see Fig. 1 for illustration of the dual correction system). Past studies have suggested that such systems generally outperform either state-update-only or rainfall-correction-only schemes (Crow and Ryu, 2009; Chen et al., 2014; Alvarez-Garreton et

Formatted: Font: Italic

al., 2016), with the rainfall correction contributing more during high-flow events and the state ~~update~~updating contributing more during low flow periods (also see Massari et al., 2018).

While these past studies ~~had~~were encouraging ~~findings~~, they applied the dual correction system only to catchment-scale, lumped hydrologic models. In this study, a semi-distributed land surface model, the Variable Infiltration Capacity (VIC) model, is implemented instead. The VIC model, compared to the previous lumped models, includes a more detailed representation of both energy and water balance processes (Liang et al., 1994; Hamman et al., 2018). The macroscale grid-based VIC also better matches the true spatial resolution of satellite SM measurements and provides a means for correcting large-scale streamflow analysis. In addition, earlier dual correction studies used previous-generation satellite products such as the Advanced Scatterometer (ASCAT) satellite SM data, the Soil Moisture Ocean Salinity (SMOS) satellite SM data and the Tropical Rainfall Measuring Mission (TRMM) precipitation data. Here, we use newer data products from the more recent Global Precipitation Measurement (GPM) mission (Hou et al., 2014) and the NASA Soil Moisture Active Passive (SMAP) mission (Entekhabi et al., 2010). Both the SMAP and GPM products provide near-real-time measurements over much of the global land surface, making them especially useful for regions with scarce ~~in-situ~~ground-based rainfall and SM observations.

The main objective of this study is to assess the effectiveness of such a dual correction system to improve streamflow simulations using ~~the latest~~recent satellite SM and precipitation products. To address this main objective, we ~~introduced a number of~~introduce methodological advances. Specifically, we 1) extended the system to provide a probabilistic streamflow estimate via ensemble ~~simulations (~~simulation and analysis techniques (note that past studies focused solely on deterministic improvement), 2) updated the rainfall correction scheme to take full advantage of the higher accuracy and ~~higher~~ temporal resolution of ~~the~~newer satellite data products, and 3) investigated the potential cross-correlation of errors in the dual system ~~and validated~~, thus validating the theoretical ~~correctness~~basis of ~~the~~our analysis system ~~design~~. These methodological contributions will be presented throughout the paper.

The remainder of this paper is organized as follows. Section 2 describes the dual correction system and our novel methodological contributions, as well as the study domain, hydrologic model, and datasets used. Results are presented in Sect. 3. Section 4 discusses ~~a few~~

~~remaining issues~~our results and ~~takeaways from the study~~identifies lessons learned, and Sect. 5 summarizes our conclusions.

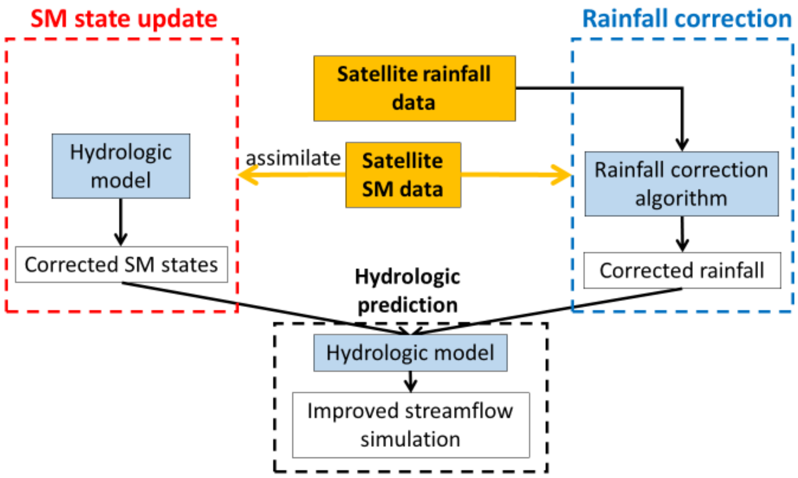

Figure 1. The dual state/rainfall correction framework applied in this study. Satellite-based soil moisture (SM) data is integrated into a hydrological simulation system via two correction schemes: 1) a standard data assimilation system to correct modeled SM states (shown in the red box on the left), and 2) a rainfall correction algorithm to correct rainfall forcing data (shown in the blue box on the right). Finally, these two contributions are combined to improve streamflow simulations (shown in the black box at the bottom).

2. Methods

2.1. Study domain

The dual state/rainfall correction system is applied in the Arkansas-Red River basin (approximately 605,000 km^2) located in the south-central United States (Fig. 2). This basin consists of the Arkansas River and the Red River, both converging eastward into the Mississippi

River. This domain has a strong climatic gradient and is wetter in the east and drier in the west (Fig. 2). The basin experiences little snow cover in winter except for the mountainous areas along its far western edge. Vegetation cover tends to be denser in the east (deciduous forest) than in the west (wooded grassland, shrubs, crops and grassland).

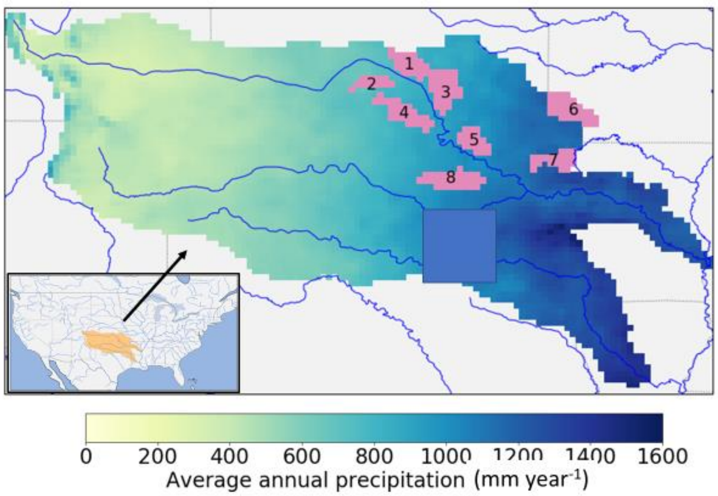

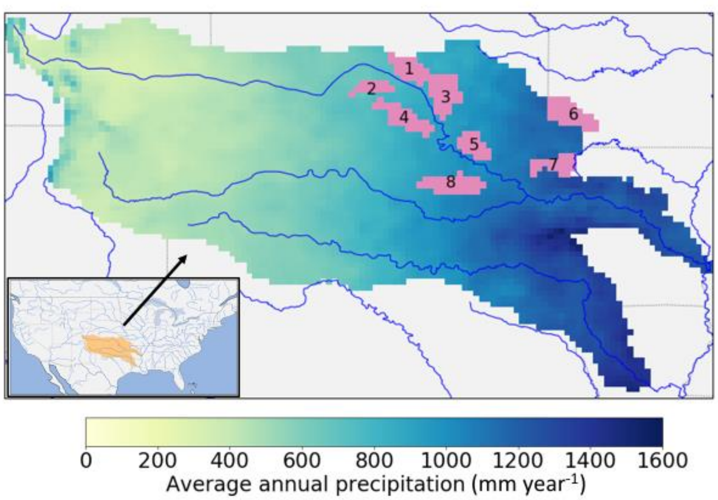

Figure 2. The Arkansas-Red River basin with climatology-averaged annual precipitation (calculated from NLDAS-2 precipitation data over 1979-2017). The pink shaded areas show the upstream sub-basins of the ~~8~~eight USGS streamflow sites evaluated in this study, with basin numbers labeled on the plot (see Table 1 for basin numbers and corresponding sites).

2.2. Data

2.2.1. SMAP satellite SM data

The SMAP mission provides SM estimates for the top 5 centimeters of the soil column, with an average revisit time of 2-3 days, a resolution of 36 km and a 50-hour data latency. Both ascending (PM) and descending (AM) retrievals from the SMAP L3 Passive product data Version 4 (O'Neill et al., 2016) from ~~Mar~~March 31, 2015 to December 31, 2017 were used in this study. A few SMAP pixels with obvious quality flaws (i.e., near-constant retrieval values) were manually masked out. The internal quality flags provided by the SMAP mission were not applied in this study to preserve the measurements in the ~~east~~eastern half of the domain, where the data quality of the entire region is flagged as unrecommended due to relatively heavy vegetation cover. The native 36-km SMAP retrievals were used throughout the study without spatial remapping or temporal aggregation.

2.2.2 GPM satellite precipitation data

The Integrated Multi-satellitE Retrievals for GPM (IMERG) Level 3 Version 05 Early Run precipitation data was used in this study (Huffman et al., 2018). IMERG merges multiple satellite observations and provides a near-global precipitation product with a spatial resolution of 0.1º (Huffman et al., 2015). ~~The~~We used the “Early Run” version of this product ~~was used in this study~~ since its short latency (4 hours) makes it suitable for near-real-time data assimilation applications. However, this short latency also prevents correction of the IMERG “Early Run” product using ground-based rain gauge observations. We aggregated the original 30-minute IMERG precipitation product to our 3-hourly modeling ~~timestep~~time step and remapped it onto our 1/8º model spatial resolution.

2.2.3. Other meteorological forcing data

Other than precipitation, the VIC model requires air temperature, shortwave and longwave radiation, air pressure, vapor pressure and wind speed as forcing inputs. These variables were ~~obtained~~taken from the 1/8º gridded North American Land Data Assimilation System Phase 2 (NLDAS-2) meteorological forcing data product (Xia et al., 2009). We aggregated the original hourly NLDAS-2 meteorological variables to the 3-hourly modeling ~~timestep~~time step.

2.2.4. Validation data

Daily streamflow data at ~~8~~eight USGS streamflow sites in the study domain (USGS, 2018) was used to evaluate the streamflow time series from the dual correction system (Fig. 2 and Table 1). These ~~8~~eight sites were selected for their lack of human regulation and their dense rain gauge coverage (Crow et al., 2017). We separately evaluated the rainfall correction scheme, in which the ~~gauge-informed NLDAS-2 precipitation data was treated as the benchmark~~NLDAS-2 precipitation data was treated as the benchmark. The NLDAS-2 precipitation data was based on daily gauge-based rainfall measurements that were disaggregated into hourly intervals using ground-based weather radar (Xia et al., 2012). NLDAS-2's reliance on gauge observations (to obtain daily rainfall accumulations) ensures that it is more reliable (in a relative sense) than the remote-sensing-only "Early Run" IMERG products used in this study. Consequently, it provides an adequate evaluation benchmark for subsequent attempts to correction IMERG.

2.3. Hydrologic modeling

We used Version 5 of the VIC model (Liang et al., 1994; Hamman et al., 2018). VIC is a large-scale, semi-distributed model that simulates various land surface processes. In this study, the VIC model was implemented in the Arkansas-Red River basin with the same setup as in Mao et al. (2019). Specifically, the model was set up at 1/8º spatial resolution with each grid cell further divided into multiple vegetation tiles via statistical distributions. Each grid cell was simulated by VIC separately using a soil column discretized into 3 vertical layers (with domain-average thicknesses of 0.10 m, 0.40 m and 0.93 m, respectively). ~~Runoff~~In VIC, runoff can be generated by fast-response surface runoff and by slow-response runoff from the bottom soil layer. All vegetation cover and soil property parameters in the model were taken from Maurer et al. (2002), which were calibrated against streamflow observations at the most downstream outlet of the combined Arkansas and Red River basins. The simulation period was from March 2015 to December 2017 when both the SMAP and GPM products are available. The VIC model was spun-up by running the period 1979-2015 twice using NLDAS-2 forcing.

The local runoff simulated by VIC at each grid cell was routed through the stream ~~channels~~network using the RVIC routing model (Hamman et al., 2017~~). RVIC~~), which is an adapted version of the routing model developed by Lohmann et al. (1996, 1998).

2.4. The dual correction system

In this section, we describe our methodological updates to the rainfall correction scheme, followed by a description of the state update scheme. Next, we describe how the two schemes are combined to produce the final ensemble streamflow analysis.

2.4.1. The SMART rainfall correction scheme updates and adaption

The Soil Moisture Analysis Rainfall Tool (SMART) rainfall correction algorithm (Crow et al., 2009; 2011; Chen et al., 2012) is based on sequential assimilation of SM measurements into ~~a simple~~an Antecedent Precipitation Index (API) model:

$$API_t = \gamma API_{t-1} + P_t \tag{1}$$

where t is a ~~timestep~~time step index; P is the original IMERG precipitation observation~~;~~ [mm]; and γ is a unitless loss coefficient. We implemented a 3-hourly version of SMART (instead of the daily version in past studies) to receive the 3-hourly IMERG rainfall input and both the ascending (PM) and descending (AM) SMAP retrievals at the correct time of day. We also extended the ensemble Kalman filter (EnKF) version of SMART introduced by Crow et al. (2011) to an ensemble Kalman smoother (EnKS), in which the API state is not only updated at ~~timesteps~~time steps when SMAP is available, but also updated during measurement gaps (see Supplemental Material Sect. S1 for mathematical details ~~of~~underlying the SMART EnKS approach). We set γ to 0.98~~ [3 hours^{-1}]~~ such that the un-corrected API time series approximately captures the dynamics of SMAP retrievals (i.e., with high correlation~~).~~; see Sect. S3 in Supplemental Material for a sensitivity analysis on γ). SMAP was rescaled to the API regime through cumulative distribution function (CDF) matching over the 2.5-year simulation period prior to assimilation. CDF matching was performed separately for SMAP AM and PM retrievals to account for their mutual systematic differences.

The SMART algorithm then uses the API increment, δ_t, to estimate the rainfall correction amount via a simple linear relation. We implemented an ensemble rainfall correction rather than the single deterministic rainfall correction used in past SMART applications:

$$P^{(j)}_{corr,t} = P^{(j)}_{pert,t} + \lambda \delta^{(j)}_t \qquad (2)$$

where the superscript *(j)* denotes the *j*th ensemble member (ensemble size $M = 32$); $P_{corr,t}$ is the corrected precipitation for time t; $P_{pert,t}$ is the perturbed IMERG precipitation; and λ is a scaling factor that linearly relates API increment to rainfall correction, which was set to a domain-constant of 0.1 [-] (see Supplemental Material Sect. ~~S2~~S4 for discussion on the choice of λ). We applied the rainfall correction only at timesteps when the original IMERG rainfall observation ~~is~~was non-zero, taking advantage of the enhanced rain/no rain detection accuracy of IMERG (Gebregiorgis et al., 2018). This tactic mitigates the ~~degradation~~spurious introduction of ~~the~~low intensity rainfall ~~estimates during low-rainfall timesteps introduced~~events by SMART ~~-~~(see also Sect. 3.1). Finally, following Crow et al. (2009; 2011), negative $P_{corr,t}$ values were set to zero, and the final corrected precipitation time series was multiplicatively rescaled to be unbiased over the entire simulation period against the original IMERG estimates~~.~~ (so that the long-term mean of the IMERG rainfall time series was preserved).

In this study, the SMART algorithm was run at each of the 36-km SMAP pixels individually. The original 0.1^{o} IMERG product was remapped to the coarser 36-km resolution prior to SMART, and the corrected 36-km rainfall was then downscaled to the VIC 1/8^{o} ~~modeling~~model resolution. In our implementation of an EnKS-based SMART system, the original IMERG precipitation was multiplicatively perturbed by log-normally distributed noise with mean and standard deviation equal to one. SMAP measurement error ranges from 0.03 to 0.045 m^3/m^3 across the domain, which was estimated from the SMAP ground validation studies (e.g., Colliander et al., 2017; Chan et al., 2017~~)~~), and its spatial distribution was set to be proportional to leaf area index (LAI) (denser vegetation cover corresponds to larger SMAP error). The API state was directly perturbed by zero-mean Gaussian noise to represent API model error. The perturbation variance was set to 0.3 mm^2 over the entire domain such that the normalized filter innovation has variance of approximately one (which is a necessary condition for the proper ~~error assumptions in~~parameterization of a Kalman filter; see Mehra (1971) and Crow and Bolten (2007)). ~~See Supplemental Material Sect. S1 for mathematical details of these~~The SMAP measurement error and the state perturbation variance are the two primary variables impacting innovation statistics. Since we had a relatively good estimate of the measurement error~~ assumptions.~~, the state perturbation level can be uniquely determined via an analysis of normalized innovation variances (Crow and van den Berg, 2010).

2.4.2. State updating via EnKF

As illustrated in Fig. 1 (the red box on the left), the SMAP SM retrievals were also assimilated into the VIC model to update model states using ~~the~~an EnKF~~ method~~. The EnKF implementation in this study generally follows Mao et al. (2019). Specifically, a 1D filter was implemented for each 36-km SMAP pixel separately and at each pixel SMAP was assimilated to update the SM states of multiple underlying finer 1/8^{o} VIC grid cells. Resolution differences between the coarser assimilation observations and finer modeling grid were accounted for via the inclusion of a spatial averaging step within the observation operator (Mao et al., 2019). Following Lievens et al. (2015; 2016) and Mao et al. ~~Only~~(2019), only the upper two layers of SM states in VIC were updated ~~during~~by the EnKF~~ (following Lievens et al. ,(2015; 2016) and Mao et al. (2019)),~~ although the bottom layer SM does respond to the update of the upper two layers through drainage~~.~~ (see Sect. S2 in Supplemental Material for mathematical details of the EnKF implemented here). An ensemble of 32 Monte Carlo model run ~~replicates~~ensembles was used ~~to represent the probabilistic estimate of corrected SM states~~for the EnKF.

The SMAP retrievals were rescaled (separately for AM and PM retrievals) to match the 2.5-year mean and standard deviation of the VIC-simulated surface-layer SM time series prior to assimilation. The error statistics of IMERG precipitation and unscaled SMAP retrievals were assumed to be the same as ~~used~~those applied in SMART (Sect. 2.4.1). ~~The~~Following Mao et al. (2019), VIC SM states ~~of all three layers~~ were directly perturbed during the EnKF forecast step by zero-mean, additive Gaussian noise with a standard deviation of 0.5 mm over the entire study domain~~ (following Mao et al. (2019)), which~~. This noise represents ~~VIC modeling errors.~~

uncertainty in VIC's ability to propagate states estimates forward in time (note that the bottom layer SM was perturbed, even though not directly updated by EnKF, to create a realistic ensemble spread for probabilistic estimates of baseflow and, thus, streamflow).

Although VIC modeling errors are likely ~~to contain~~spatially auto-correlated, we tested whether accounting for spatial ~~auto-~~correlation~~, consideration of this~~ improved filter performance. Since it did not ~~result in~~ significantly ~~better filter performance~~improve the results, we did not account for spatial correlation in our ~~case and therefore not implemented here.~~EnKF implementation. This finding is consistent with Gruber et al. (2015) ~~which~~who described the limited benefit of ~~a~~ 2-D ~~filter~~filtering, versus a 1-D baseline, when assimilating distributed SM retrievals into a land surface model. We will further discuss this point in Sect. 4.

Formatted: Indent: First line: 0.5"

2.4.3. Combining the state update and the rainfall correction schemes

The ensemble of updated model states and the corrected rainfall forcing were combined to produce final streamflow ~~results~~estimates (black box in the bottom of Fig. 1). We first randomly paired ensemble members of corrected rainfall and updated VIC states and selected 32 such pairs to balance competing considerations of computational cost and statistical stability. For each pair, the VIC model was re-run with the updated states inserted sequentially over time and forced by the corrected rainfall. Other meteorological forcings were kept unchanged. The runoff output from VIC for each pair was then routed to the gauge locations, resulting in an ensemble of basin-outlet streamflow time series~~ for evaluation.~~. To further separate the relative contribution of the state update and the rainfall correction schemes to overall streamflow improvement, two additional streamflow simulations were performed. The first was the "state-updated streamflow" case, where VIC was re-run with the updated states and forced by the original IMERG precipitation. The resulting streamflow reflects only the impact of state updating on streamflow simulations. The second was the "rainfall-corrected streamflow" case, where VIC was forced by the SMART-corrected rainfall ensemble but without inserting the updated states. The resulting streamflow reflects only the effect of SMART rainfall correction.

~~Although the~~The EnKF state update and SMART rainfall correction schemes were ~~performed separately with no feedback~~executed independently to ~~each other to mitigate~~

minimize the risk of cross-correlated error (Crow et al., 2009~~), error correlation still~~). In particular, note that VIC state estimates created using SMART forcing – see the black “Hydrologic prediction” box in Fig. 1 – were not fed back into the EnKF state update analysis. Nevertheless, cross-correlated error in (EnKF) state and (SMART) rainfall estimates potentially ~~exists in the dual system~~may still be present since the two schemes are informed by the same SM measurement ~~data~~time series. Such cross-correlated error could~~ potentially be amplified when combining the two schemes and degrading~~, in turn, degrade the quality of probabilistic streamflow estimates. In fact, due to this concern, Massari et al. (2018) intentionally avoided combining the state and rainfall correction schemes~~ due to this concern.~~. To further investigate this risk, we performed a set of synthetic experiments where we compared probabilistic streamflow estimates obtained via the following two scenarios: 1) a single set of synthetically generated SM measurements ~~were~~ assimilated into the state and rainfall correction schemes, mimicking the ~~real~~original dual correction system; 2) two separate sets of SM measurements with mutually independent errors ~~were~~ assimilated separately into the two schemes, thereby explicitly avoiding error cross-correlation in the system. Results show that the two scenarios achieve very similar streamflow correction performance~~. This suggests that it is safe to assimilate a single SM measurement product into both schemes without significantly degrading the final streamflow performance (see Sect. S3~~ and, therefore, minimal risk of degraded streamflow estimates (see Sect. S5 in Supplemental Material).

2.5. Evaluation strategies and metrics

We evaluated the rainfall correction results in addition to the dual-corrected streamflow results in terms of both deterministic and probabilistic metrics.

The 1/8^{o} gauge-informed NLDAS-2 precipitation data was remapped to the 36-km SMART resolution grid as the benchmark for evaluating rainfall. Deterministically, the ensemble-mean SMART-corrected rainfall was compared to the original IMERG precipitation (remapped to 36 km), and its improvement was evaluated in terms of: 1) time series correlation coefficient (*r*~~) of time series;~~); 2) percent error reduction (PER) in terms of the root-mean-squared error (RMSE); 3) ~~Categorical~~additional categorical skill metrics, including false alarm ratio (FAR), probability of detection (POD) and threat score (TS) (Wilks, 2011; Crow et al., 2011; Chen et al., 2012; Brocca et al., 2016). Probabilistically, the normalized ensemble skill (NENSK) was calculated, which measures the ensemble-mean error normalized by ensemble spread:

$$NENSK = \frac{ENSK}{ENSP} \tag{3}$$

where the ensemble skill (ENSK) is the temporal mean of ensemble-mean squared error, and the ensemble spread (ENSP) is the temporal mean of ensemble variance (De Lannoy et al., 2006; Brocca et al., 2012; Alvarez-Garreton et al., 2014; Mao et al., 2019). ~~Ideally, if~~If an ensemble of time series correctly ~~represent~~represents the uncertainty of an analysis, NENSK ~~should be 1~~will equal one (Talagrand et al., 1997; Wilks, 2011). NENSK > 1 indicates an under-dispersed ensemble while NENSK < 1 indicates an over-dispersed ensemble. For all metrics, precipitation datasets were aggregated to multiple temporal accumulation periods (the native 3-hour period without aggregation; 1-day; 3-day) for evaluation at different time scales.

The dual-corrected streamflow was evaluated at the ~~8~~outlet of the eight USGS ~~sites~~sub-basins shown in Fig. 2. Deterministically, the ensemble-median corrected streamflow was compared to the baseline streamflow, or the so-called "open-loop" streamflow, which is simply the single VIC simulation forced by IMERG precipitation without any correction, in terms of 1) PER; and 2) the Kling-Gupta efficiency (KGE) (Gupta et al. 2009~~) which~~). The latter combines the performance of correlation, variance and bias. Ensemble-median instead of ensemble-mean streamflow was used for more stable evaluation results in the case of a skewed streamflow ensemble caused by model nonlinearity. ~~Probabilistically~~In addition to ensemble-median evaluations, NENSK was calculated for the entire streamflow ensembles.

3. Results

3.1. SMART rainfall correction

3.1.1. The impact of SMART methodological choices

Figure 3 shows the rainfall improvement in terms of correlation coefficient *r* based on both an EnKS- (the left column) ~~compared to~~and EnKF-based (the right column~~).~~)

implementation of SMART. For EnKF results, both δ and P in Eq. (2) were aggregated to 3-day windows prior to correction to ensure SM data availability in every correction window~~.~~ (and the 3-day correction was subsequently downscaled to 3-hour time steps uniformly). Overall, the EnKF implementation results in less r improvement than the EnKS ~~overall~~implementation, which confirms the benefit of applying SMART using a smoothing approach.

The impact of our (previous choice~~ of only correcting~~) to update rainfall only at non-zero IMERG ~~timesteps~~time steps is ~~demonstrated by the~~examined via domain-median categorical metrics (Fig. 4). ~~If~~When we correct rainfall every ~~timestep is corrected~~time step (Fig. 4 Column 1), FAR is largely degraded (by 0.1 – 0.4) at low rainfall event thresholds especially with shorter accumulation periods (3-hour and 1-day; see Fig. 4a). This is likely due to ~~the issue of~~ SMART misinterpreting SM retrieval noise as small rainfall ~~corrections~~events (Chen et al., 2014). POD is improved at these low thresholds (Fig. 4b), but not enough to compensate for the large FAR degradation. Therefore, TS, which accounts for both false alarms and missed events, is also degraded at low thresholds (by as large as 0.2 at 3-hourly). In contrast, when we only correct rainfall at non-zero IMERG ~~timesteps~~time steps (Fig. 4 Column 2), the FAR degradation is much less (note the different y-axes in the two columns in Fig. 4). While ~~it~~this approach does sacrifice POD at low thresholds (Fig. 4e), the overall TS for 1-day and 3-day aggregation is improved ~~over~~for most ~~of the~~ event thresholds, especially ~~at~~the higher ones. As mentioned in Sect. 2.4.1, one possible reason for the success of this SMART choice is~~ likely due to~~ the improved rain/no rain detection quality of the baseline IMERG precipitation product, which was found to have ~~superior~~improved miss-rain, false-rain and hit rate relative to older TRMM TMPA-RT products over the Continental U.S. (Gebregiorgis et al., 2018). It is thus ~~more~~ beneficial to retain ~~the~~ IMERG's rain/no rain detection ~~than~~skill and not subject it to ~~use~~ SMART~~ to correct it~~-based correction.

With regards to binary rain/no-rain determination, one strategy for mitigating FAR problems is to arbitrarily set a (greater than zero) minimum accumulation threshold that must be exceeded for an event to be registered. To this end we carried out a sensitivity analysis to examine the impact of using a non-zero rain/no rain threshold versus our baseline assumption of a zero threshold. However, this analysis was unable to isolate an optimized threshold value for distinguishing rain/no rain cases. Instead, a continuous trade-off exists between POD and FAR at different rainfall thresholds. However, a zero rain/no rain threshold does appear slightly beneficial for PER and the correlation coefficient improvement (see Sect. S6 in Supplemental Material).

3.1.2. Rainfall correction evaluation

After rainfall correction at 1-day and 3-day accumulation periods, PER exhibits a domain-median error reduction of ~8% (Fig. 5 Column 1). The PER improvement is consistent with the improvement of the categorical metrics at high-event thresholds (Fig. 4 Column 2), since PER is more sensitive to high rainfall values. Three-hourly PER shows little improvement (Fig. 5a), suggesting that the deterministic correction is more effective at an accumulation period that more closely matches the SMAP retrieval interval. The same finding can also be drawn from the correlation and categorical results (Fig. 3 Column 2 and Fig. 4 Column 2).

~~Overall, SMART improves the IMERG rainfall product, but the improvement is generally smaller than found in previous SMART studies, especially in terms of correlation *r* (domain-median improvement of 0.01 to 0.02). The relatively smaller improvement is likely due to the improved accuracy of the baseline IMERG precipitation product. Table 2 summarizes the past SMART studies in literature, including the baseline and benchmark rainfall products, the SM product assimilated, baseline correlation *r* and its improvement, and baseline RMSE and its reduction (PER). Over the past decade, the quality of the baseline satellite-derived rainfall product has improved considerably, from TRMM 3B40-RT used in Crow et al.~~ Overall, the correlation coefficient improves more in the western part of the domain, which is likely attributable to the better quality of SMAP retrievals in the lightly vegetated western portion of the basin. However, RMSE is reduced more in the eastern part of the domain, which is likely due to the increased frequency of large rainfall events in this region, and SMART's tendency to be more effective for the correction of moderate-to-large precipitation events. Note that SMART rainfall correction cannot be evaluated in terms of overall bias, since – like all SM data assimilation systems - the SMART algorithm rescales the corrected time series back to the uncorrected mean prior to its evaluation~~(2009) and Crow et al. (2011) with *r* = ~0.5, to TRMM 3B42-RT used in Brocca et al. (2016) with *r* = ~0.6 – 0.7, to IMERG used in our study with *r* over 0.8. Gebregiorgis et al. (2018) also used a direct comparison study to show the improved accuracy of IMERG relative to TRMM over the Continental U.S. in terms of correlation, RMSE,~~

~~bias and categorical metrics. The marginal value of SMART is known to decrease as a function of increased baseline rainfall accuracy (Crow et al., 2011). Although SMAP presumably provides more reliable SM measurements than the older satellite SM products used in previous SMART applications, its benefit does not appear sufficient to substantially correct the current generation of satellite-derived rainfall products. The high correlation may also be approaching that of the NLDAS-2 rainfall benchmark (which itself does not have perfect accuracy), thus undermining our ability to detect improvements in SMART rainfall estimates~~.

~~Finally, the~~The probabilistic metric NENSK (Fig. 5 Column 2) is less than one for most of the domain at a 3-hour ~~timestep~~time step, indicating an over-dispersed ensemble on average. However, when evaluating at 1-day and 3-day accumulation periods, NENSK is closer to one, indicating a better representation of the uncertainty of the rainfall estimates. As we aggregate over longer accumulation windows (e.g., 3-day), NENSK becomes slightly greater than ~~1~~one (i.e., under-dispersed ensemble), since the SMART algorithm ~~only~~ assumes only a random rainfall error but ~~not~~no systematic bias~~, and therefore~~. As a result, it slightly underestimates the uncertainty range over longer-term periods. Ensemble rainfall tends to be under-dispersed on the west edge of the domain with low rainfall, indicating that we are underestimating rainfall uncertainty in this region.

In summary, SMART ~~is able to use the~~successfully uses SMAP SM retrievals to correct IMERG rainfall ~~at~~during relatively larger events, with slight to moderate deterministic improvement. However, SMART correction is less successful for small rainfall events and can even lead to slight degradation. The correction is more effective, and the ensemble representation is better, when rainfall estimates are temporally aggregated to periods consistent with SMAP retrieval intervals (i.e., 1-day to 3-day accumulation periods~~), while the raw 3-hourly correction is less successful.~~).

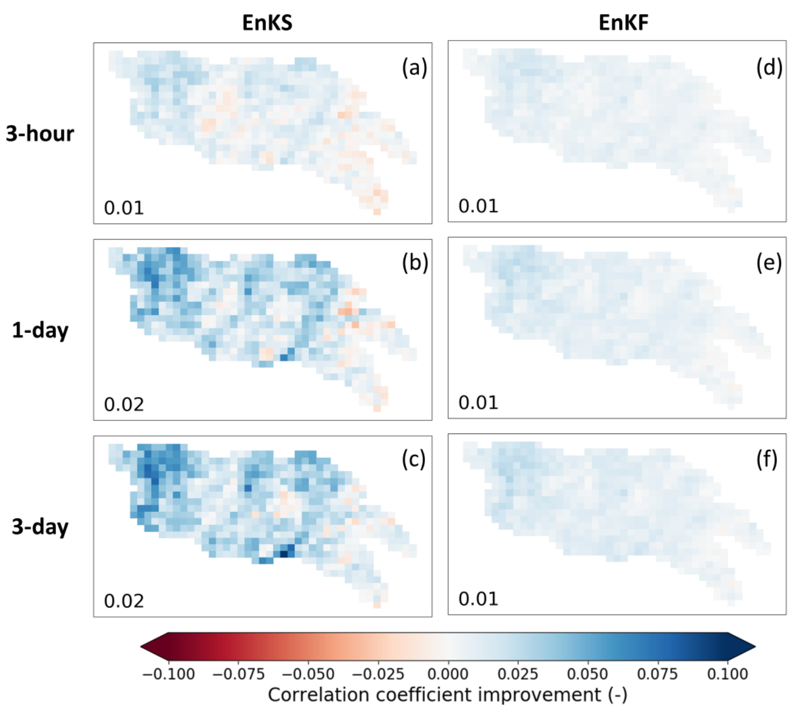

Figure 3. Maps of correlation coefficient improvement after SMART rainfall correction~~.~~ (i.e., improvement of correlation with respect to NLDAS-2 benchmark rainfall realized upon implementation of SMART). The left column shows the SMART EnKS experiments (*a*, *b*, *c*), and the right column shows the EnKF experiments (*d*, *e*, *f*). Each row shows results based on different temporal accumulation ~~period:~~periods (i.e., 3-hourly, 1-day and 3-day aggregation, respectively~~.~~). The number on the lower left corner of each subplot shows the domain-median correlation improvement.

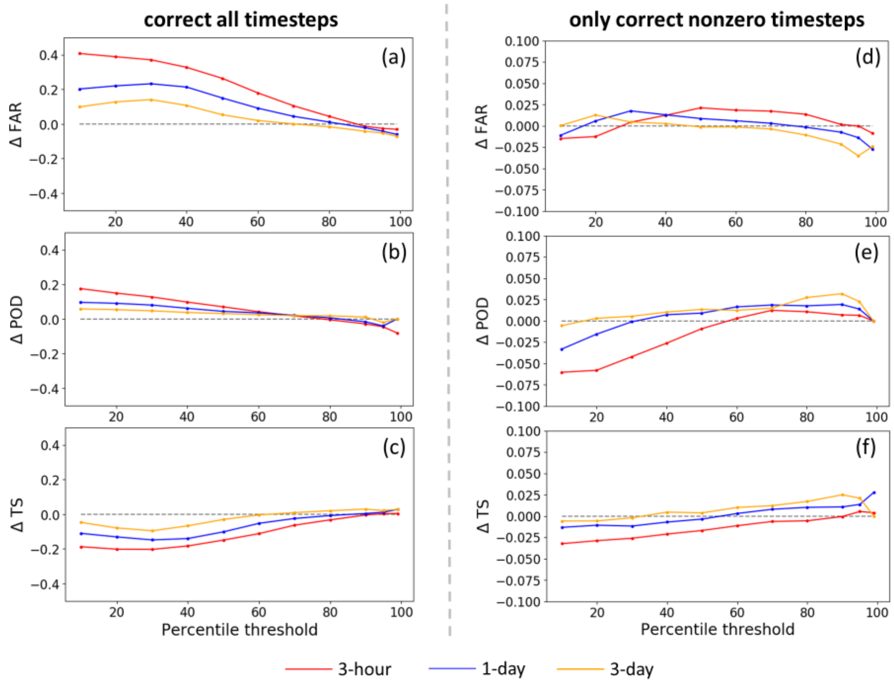

Figure 4. Change in categorical metrics (FAR, POD and TS) before and after SMART correction for 3-hourly, 1-day and 3-day accumulation periods. Metrics at different ~~event~~rainfall thresholds are shown on the *x* axis~~.~~ (e.g., the 80th percentile means that an event is defined as exceeding the 80th percentile of non-zero rainfall accumulation over the listed time accumulation period). The left column (*a*, *b*, *c*) is for SMART with rainfall corrected at all ~~timesteps~~time steps; the right column (*d*, *e*, *f*) is for SMART with rainfall corrected only at non-zero ~~timesteps~~time steps. Note that the y-axis range is different for the two columns.

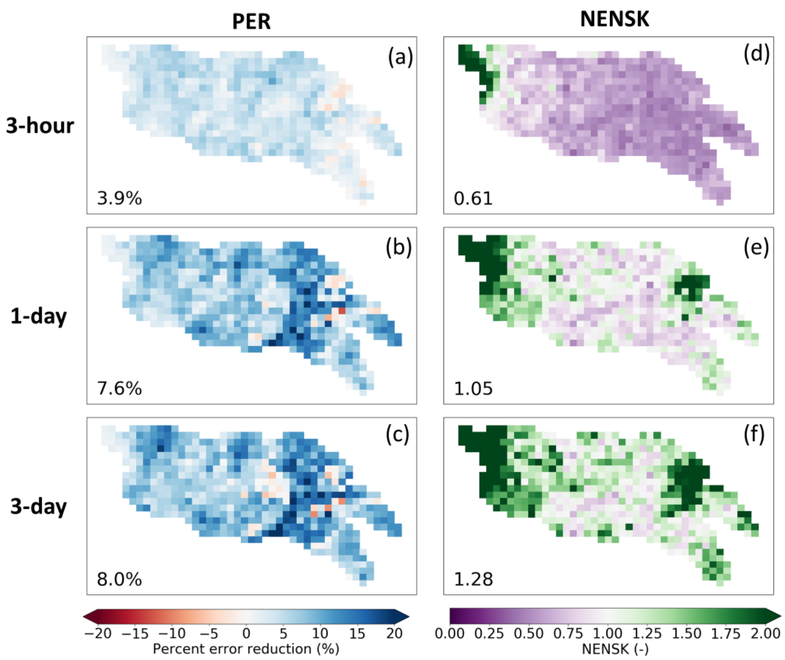

Figure 5. Maps of SMART rainfall correction results (with $\lambda = 0.1$, EnKS, and rainfall corrected only ~~at~~during time steps with non-zero ~~timesteps~~rainfall). Each column shows the following metrics, respectively: percent RMSE reduction (PER) (*a*, *b*, *c*), and ensemble NENSK (*d*, *e*, *f*). Each row shows results based on different temporal accumulation period: 3-hourly, 1-day and 3-days, respectively. The number ~~on~~in the lower left corner of each subplot shows the domain-median statistic.

3.2. Streamflow from the dual correction system

3.2.1. Evaluation of streamflow improvement

The final daily streamflow performance from the dual correction system is listed in Table ~~3~~2 (the "*dual*" columns) for each sub-basin. Overall, streamflow estimates are improved but with large variability across sub-basins. Specifically, PER ranges from approximately 6% to 34% and KGE improvement ranges from slightly negative to +0.95 across all sub-basins. ~~If using the~~

~~open-loop KGE (listed in Table 3) as a measure of~~ For sub-basins with better baseline streamflow performance ~~without any correction, we observe that at sub-basins with better open-loop streamflow simulations (~~(as measured by KGE, i.e., the Ninnescah, Walnut and Chikaskia~~,~~ ~~all with positive baseline KGE~~ sub-basins), the relative improvement after the dual correction is generally smaller.

Table ~~3~~2 also summarizes the streamflow improvement from each of the correction schemes alone (i.e., the "*state update only*" and "*rainfall correction only*" columns). For sub-basins with relatively better open-loop model performance ~~(the three with positive KGE as well as the Little Arkansas with slightly negative baseline KGE),~~, the contribution of state updating ~~in general~~generally surpasses that of rainfall correction. Conversely, at sub-basins with relatively poorer open-loop model performance (i.e., the Bird, Spring, Illinois and Deep sub-basins), streamflow improvement is primarily attributable to the SMART rainfall correction ~~scheme~~.

3.2.2. Impact of rainfall forcing error

To further understand the relationship between open-loop simulation performance, rainfall forcing error and correction performance, we forced the VIC model by the NLDAS-2 benchmark rainfall (without state update). The subsequent streamflow improvement level is assumed to approximate the maximum improvement achievable ~~by~~via rainfall correction alone (Table ~~3~~2 "*NLDAS2-forced*" columns). While almost all sub-basins show ~~an obvious~~ streamflow improvement simply by switching to ~~the~~ NLDAS-2 rainfall forcing, the improvement is ~~larger at~~especially large for sub-basins with poorer open-loop streamflow~~. For example, at the four sub-~~ estimates. In these basins ~~with worse open-loop streamflow~~, PER is over 65% and the negative ~~open-loop~~ KGE for the open loop case improves to near zero or positive~~.~~ values for the NLDAS-forced case. This suggests that ~~the~~, despite advances in the quality of remotely sensed rainfall data products, poor open-loop streamflow simulations at these sub-basins are still largely ~~caused by the~~attributable to poor-quality IMERG rainfall forcing~~. While the state update is still beneficial at these sub-~~ error. In these basins, ~~the SMART~~SM-based rainfall correction scheme ~~is particularly~~ can potentially play an important role in improving VIC streamflow estimates. Unfortunately, this potential is not always realized. Note how the SMART-based rainfall-correction-only case generally fails to match NLDAS-forced case in the Spring, Illinois and

Deep sub-basins (Table 2). This is likely because these basins are located in relatively high biomass areas where SMAP retrievals (and thus SMART corrections) are less accurate.

In contrast, the sub-basins with better open-loop streamflow results (i.e., the Ninnescah, Walnut and Chikaskia sub-basins) demonstrate ~~a reduced capability of~~less streamflow improvement when switching to the NLDAS-2 rainfall forcing. The sub-basin with best (IMERGE-forced) open-loop streamflow results, Chikaskia, even experiences ~~smaller streamflow improvement~~a small degradation when forced by the NLDAS-2 rainfall ~~than when forced by SMART-corrected rainfall~~ (Table ~~3). One possible reason is~~2). This suggests that the NLDAS-2 benchmark rainfall at this sub-basin is not obviously superior than the IMERG baseline. ~~Therefore, switching to the NLDAS-2 rainfall forcing does not benefit streamflow much, but~~Nevertheless, SMART is still able to extract information from SMAP and slightly correct IMERG rainfall and subsequent streamflow estimates.

3.2.3. Impact of model parameterization

The dual correction scheme presented in this study is designed to ~~only~~ correct only the random error ~~existing~~present in ~~the~~a hydrologic simulation system~~, but~~. It does not correct systematic error or overall bias. Figure 6 shows example time series of the open-loop, USGS-observed and dual-corrected streamflow at three sub-basins (the Chikaskia, Deep and Illinois) with various levels of open-loop performance. ~~It is readily apparent from the time series that, although~~Although the dual system often nudges the simulated streamflow in the correct direction (especially during high-flow periods) and results in overall improved evaluation statistics, ~~obvious~~ systematic error (in the model process representation as well as rainfall forcing) clearly exists. This systematic error, although difficult to quantify, cannot be corrected by the data assimilation approach discussed here. The NENSK statistic partly reflects such systematic error. NENSK is significantly above one at most sub-basins, indicating an under-dispersed ensemble on average. In other words, at most sub-basins the ensemble spread created by the dual system only represents the random uncertainty around the open-loop streamflow~~, but not the~~ and neglects systematic error ~~which~~that accounts for ~~much~~a significant fraction of ~~the~~ total streamflow error.

The level of systematic error is tied closely to the quality of the hydrologic model parameters~~,~~ often estimated through calibration. The VIC parameters used in this study were taken from Maurer et al. (2002) and derived based on streamflow at the outlets of large basins. To further examine the effect of systematic error on data assimilation, we ~~instead~~ calibrated the model parameters for the ~~8~~eight sub-basins separately using streamflow acquired from the USGS (Table 1). Specifically, VIC parameters that control infiltration, soil conductivity and baseflow generation as well as the recession rate of the grid-cell-scale unit hydrograph in RVIC were calibrated using the MOCOM multi-objective autocalibration method (Yapo et al., 1998). Basin-constant parameters were calibrated toward USGS streamflow time series during 2015 to 2017 (forced by the baseline IMERG precipitation) to optimize daily KGE and monthly bias. Only a subset of the ~~8~~eight sub-basins ~~were able to achieve~~achieved better-than-open-loop streamflow results via this traditional calibration method, due mainly ~~due~~ to the relatively large IMERG forcing error ~~at~~present in some sub-basins that ~~makes~~prevents the calibration scheme ~~incapable of~~from finding an improved parameterization. Figure 7 shows three example sub-basins (i.e., Chikaskia, Deep and Illinois) with relatively good calibration ~~outcome as demonstration.~~outcomes. Comparing Fig. ~~6 and~~7 to Fig. ~~7, all three sub-basins exhibit a similar or smaller magnitude of~~ 6, we observe that the streamflow ~~correction after~~improvement achieved by parameter calibration~~. While a good calibration itself can~~ (i.e., systematic error reduction) alone is as, or more, important than that achieved by data assimilation (via random error reduction) in all three sub-basins. In both cases (i.e., the default and calibrated VIC parameters), NENSK is significantly ~~improve baseline performance, a poor calibration does not degrade (and sometimes even benefit) the relative added value of the dual correction~~above one, indicating that we underestimate the streamflow simulation uncertainty when only random errors are considered.

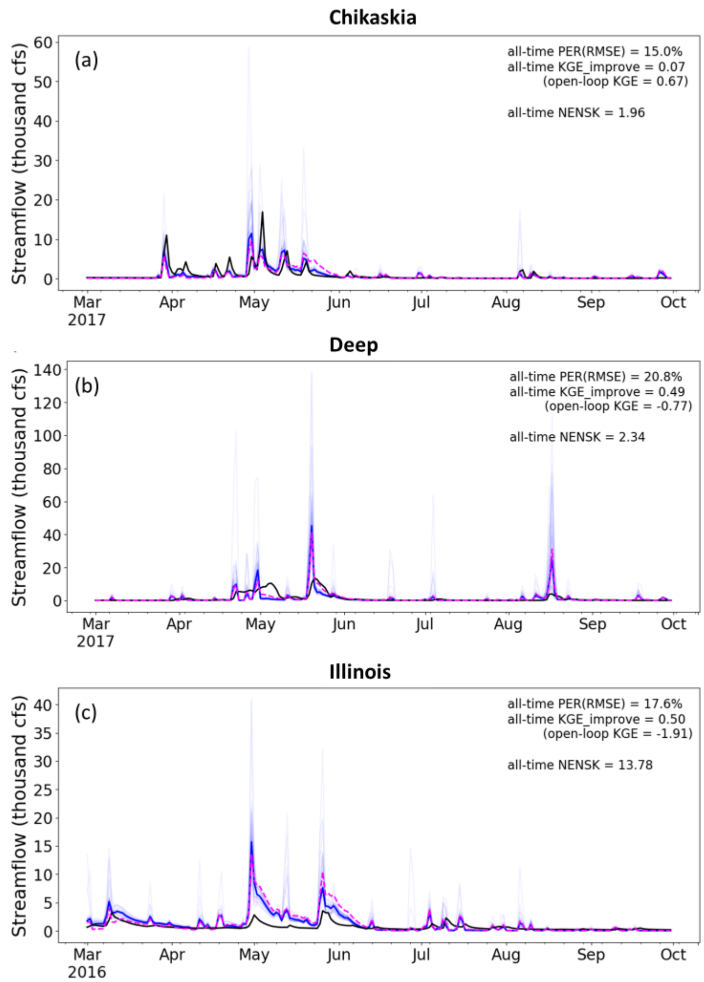
Chikaskia
(a)
all-time PER(RMSE) = 15.0%
all-time KGE_improve = 0.07
(open-loop KGE = 0.67)
all-time NENSK = 1.96
Streamflow (thousand cfs)
Mar 2017
Apr
May
Jun
Jul
Aug
Sep
Oct
Deep
(b)
all-time PER(RMSE) = 20.8%
all-time KGE_improve = 0.49
(open-loop KGE = -0.77)
all-time NENSK = 2.34
Streamflow (thousand cfs)
Mar 2017
Apr
May
Jun
Jul
Aug
Sep
Oct
Illinois
(c)
all-time PER(RMSE) = 17.6%
all-time KGE_improve = 0.50
(open-loop KGE = -1.91)
all-time NENSK = 13.78
Streamflow (thousand cfs)
Mar 2016
Apr
May
Jun
Jul
Aug
Sep
Oct

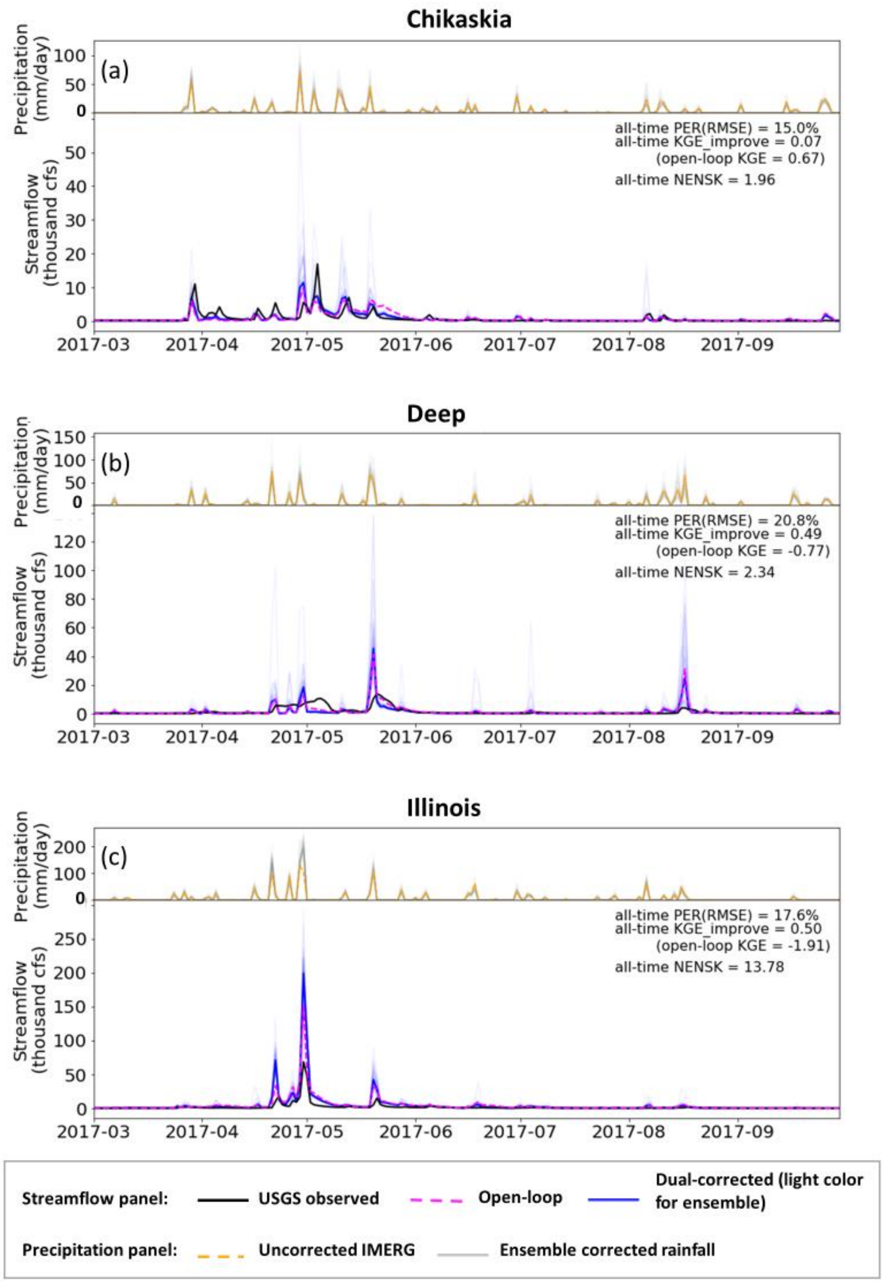
Chikaskia
(a)
Precipitation (mm/day)
Streamflow (thousand cfs)
all-time PER(RMSE) = 15.0%
all-time KGE_improve = 0.07
(open-loop KGE = 0.67)
all-time NENSK = 1.96
Deep
(b)
Precipitation (mm/day)
Streamflow (thousand cfs)
all-time PER(RMSE) = 20.8%
all-time KGE_improve = 0.49
(open-loop KGE = -0.77)
all-time NENSK = 2.34
Illinois
(c)
Precipitation (mm/day)
Streamflow (thousand cfs)
all-time PER(RMSE) = 17.6%
all-time KGE_improve = 0.50
(open-loop KGE = -1.91)
all-time NENSK = 13.78
2017-03 2017-04 2017-05 2017-06 2017-07 2017-08 2017-09
Streamflow panel:
USGS observed
Open-loop
Dual-corrected (light color for ensemble)
Precipitation panel:
Uncorrected IMERG
Ensemble corrected rainfall

Figure 6. Example time series of streamflow results from the dual correction system. In the lower panel, ~~B~~b*lack line*: USGS observed streamflow; *magenta line*: baseline VIC simulation; *light blue lines*: ensemble updated streamflow results; *solid blue line*: ensemble-mean updated streamflow. In the upper panel, *orange line*: uncorrected IMERG rainfall aggregated to the sub-basin-average; *light grey lines*: ensemble corrected rainfall. Only part of the simulation period is shown for clear display~~. Statistics~~; however, statistics shown on each panel are based on the entire simulation period (approximately 2.5 years).

Formatted: Font: Italic

Formatted: Font: Italic

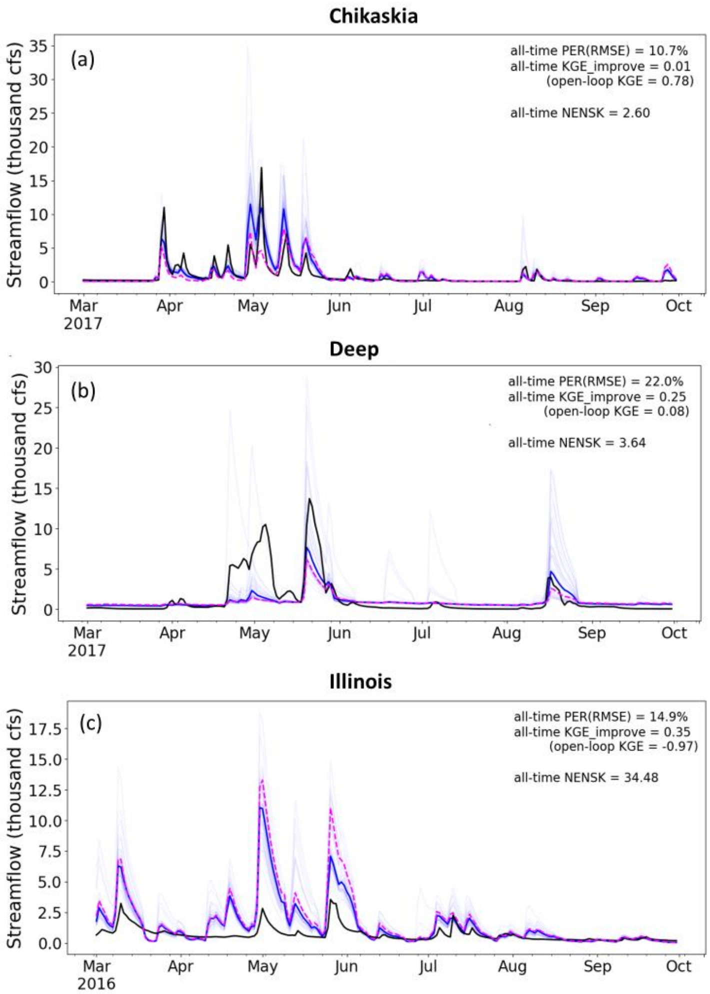
Chikaskia
(a)
all-time PER(RMSE) = 10.7%
all-time KGE_improve = 0.01
(open-loop KGE = 0.78)
all-time NENSK = 2.60
Streamflow (thousand cfs)
Mar 2017
Apr
May
Jun
Jul
Aug
Sep
Oct
Deep
(b)
all-time PER(RMSE) = 22.0%
all-time KGE_improve = 0.25
(open-loop KGE = 0.08)
all-time NENSK = 3.64
Streamflow (thousand cfs)
Mar 2017
Apr
May
Jun
Jul
Aug
Sep
Oct
Illinois
(c)
all-time PER(RMSE) = 14.9%
all-time KGE_improve = 0.35
(open-loop KGE = -0.97)
all-time NENSK = 34.48
Streamflow (thousand cfs)
Mar 2016
Apr
May
Jun
Jul
Aug
Sep
Oct

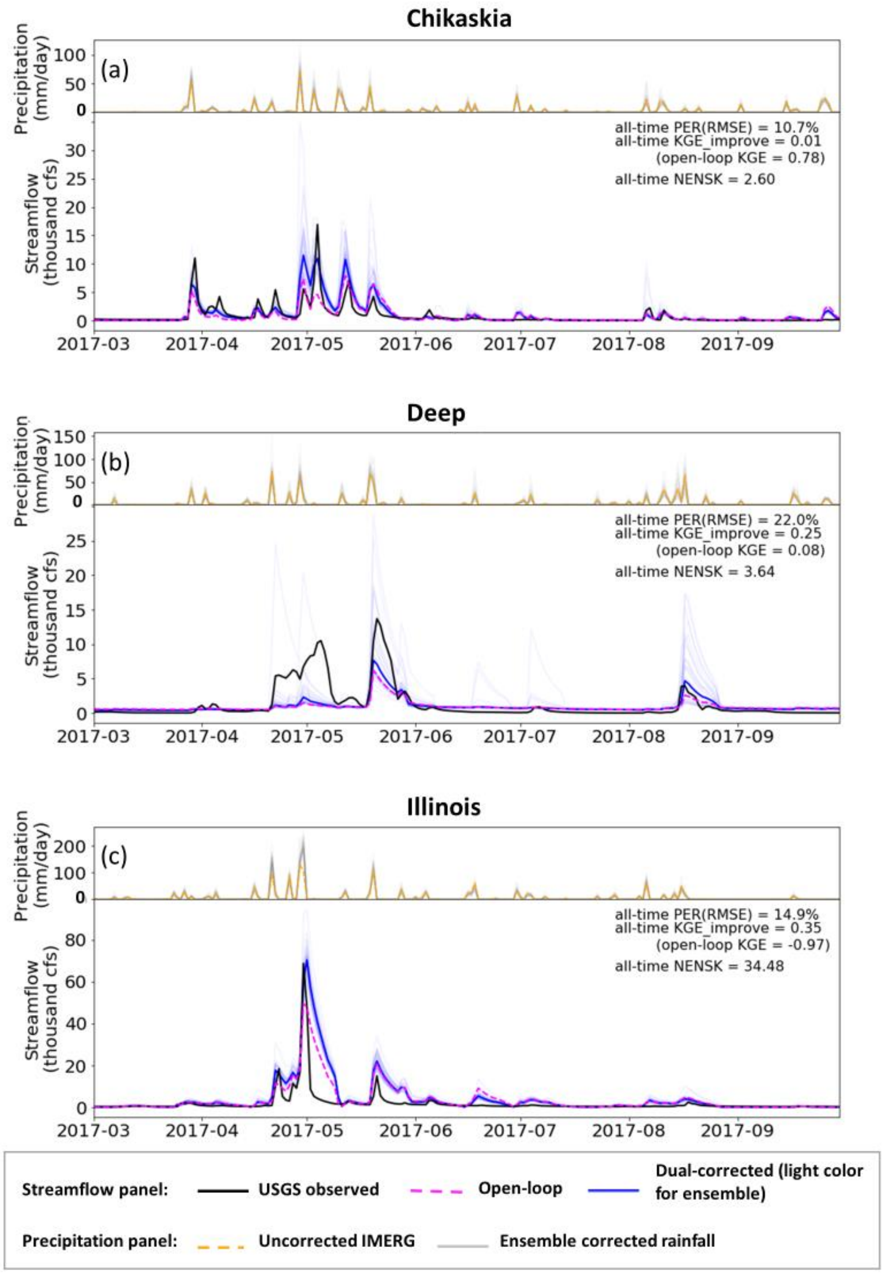

Chikaskia
(a)
Precipitation (mm/day)
Streamflow (thousand cfs)
all-time PER(RMSE) = 10.7%
all-time KGE_improve = 0.01
(open-loop KGE = 0.78)
all-time NENSK = 2.60
Deep
(b)
all-time PER(RMSE) = 22.0%
all-time KGE_improve = 0.25
(open-loop KGE = 0.08)
all-time NENSK = 3.64
Illinois
(c)
all-time PER(RMSE) = 14.9%
all-time KGE_improve = 0.35
(open-loop KGE = -0.97)
all-time NENSK = 34.48
2017-03
2017-04
2017-05
2017-06
2017-07
2017-08
2017-09
Streamflow panel:
USGS observed
Open-loop
Dual-corrected (light color for ensemble)
Precipitation panel:
Uncorrected IMERG
Ensemble corrected rainfall

Figure 7. ~~Time series of simulated open-loop, corrected and observed streamflow at three example sub-basin outlets with~~Same as Fig. 6, but calibrated VIC model parameters.~~ All lines and notations are the same as in Fig. 6.~~

Formatted: Font: Bold

4. Discussion

4.1. SMART rainfall correction

Overall, SMART improves the IMERG rainfall product (see Figures 3 to 5); however, the magnitude of improvement is somewhat smaller than that found in previous studies, especially in terms of correlation *r* (domain-median improvement of 0.01 to 0.02). Table 3 summarizes results from past studies that applied remotely sensed SM to correct rainfall time series. Over the past decade, the quality of the baseline satellite-derived rainfall product has improved considerably, from the TRMM 3B40-RT product used by Crow et al. (2009) and Crow et al. (2011) with r = ~0.5, to the TRMM 3B42-RT product used by Brocca et al. (2016) with r = ~0.6 – 0.7, to the IMERG product used in our study with r over 0.8. This tendency is confirmed by Gebregiorgis et al. (2018) who demonstrated the improved accuracy of IMERG relative to TRMM over the Continental U.S. in terms of correlation, RMSE, bias and categorical metrics. This improvement is relevant here because the marginal value of data assimilation tends to decrease as the skill of the background land surface model increases (Reichle et al., 2008; Qing et al., 2011; Bolten and Crow, 2012; Dong et al., 2019). Since SMART is fundamentally a data assimilation approach, the added value of its SM-based correction tends to *decrease* as the accuracy of the baseline product (it is correcting) increases. This tendency, previously noted in Crow and Ryu (2009) and Crow et al. (2011), is clearly illustrated in Table 3. Therefore, large improvement over time in the quality of satellite-based rainfall products appears to have partially undercut the value of SM-based rainfall correction. It should be noted that the SM/rainfall correction algorithms applied in Table 3 differ slightly. However, Brocca et al. (2016) found comparable performance even when inter-comparing very different rainfall correction approaches, suggesting that the various studies listed in Table 3 are relatively inter-comparable.

4.2. Dual correction for streamflow

Although we applied the dual correction system to the entire Arkansas-Red basin, we selected ~~8~~only eight smaller sub-basins for our streamflow evaluation due to the limited availability of unregulated streamflow observations at basin outlets. ~~Additional research is needed to fully investigate the impact of error spatial correlation on downstream streamflow performance before extending our findings to large-scale river systems. Specifically, while a 1-D filter with spatially white model representation error may be appropriate for small-basin correction, ignoring the spatial correlation structure of errors could potentially have a more profound impact on the correction performance at large river outlets where streamflow originates from runoff from a large number of grid cells. A number of~~While~~ studies have investigated the effects of spatial error patterns in hydrologic data assimilation. For example, Reichle and Koster (2003) investigated the impact of spatial error correlation in the model SM states on its assimilation performance; Gruber et al. (2015) examined the impact of a 2-D filter with spatially auto-correlated error versus a 1-D filter on SM updating quality; Pan et al. (2009) and Pan and Wood (2009; 2010) evaluated the surface SM assimilation performance with VIC by comparing a 1-D filter, a 2-D filter and a multiscale autoregressive filtering approach, as well as considering spatial and temporal structure of precipitation error. However, these studies focused exclusively on the performance of SM simulations. Direct assessment of the impact of spatial error patterns on the routed streamflow results is needed, especially from a probabilistic perspective since the ignorance of spatial error patterns may potentially cause error cancelation at large outlets and therefore incorrect ensemble representation of uncertainty.~~

~~Nevertheless, this study leads to a number of valuable insights. We have shown that~~ the dual correction approach ~~is able to correctly nudge~~generally improved VIC streamflow ~~simulation~~estimates, especially during relatively high flow events in areas with poor IMERG data~~. However~~, the magnitude of this correction ~~is generally small for two~~was relatively modest. Results in Sect. 3 indicated three general reasons for this. First, the latest generation of satellite rainfall products (e.g., IMERG) has significantly improved precision compared to its predecessors. The already high-quality rainfall estimates are more difficult for SM retrievals to contribute substantial rainfall correction skill~~.~~ (see discussion in Sect. 4.1 above). Second, the dual correction approach is designed to correct only the zero-mean random error component in the total streamflow error but not systematic error or bias. However, systematic error sources, typically associated with inaccurate model structure and/or parameterization and large rainfall bias, can account for a significant fraction of overall streamflow error~~.~~ (Sect. 3.2.3). The existence of systematic error is particularly problematic from a probabilistic perspective, since the ensemble streamflow produced by the dual system only represents random error, and therefore largely underestimates simulation uncertainty. Finally, in certain sub-basins (i.e., the Bird, Spring, Illinois and Deep sub-basins) where VIC streamflow is substantially degraded by random error in IMERG data products, SMART-based dual correction often underperformed due to the reduced accuracy of SMAP-based rainfall correction in eastern areas of the domain with relatively dense biomass (see Fig. 3).

In addition to these factors, additional research is needed to fully investigate the impact of several simplifications applied in the dual correction data assimilation system. For example, the impact of error spatial correlation on downstream streamflow performance should be fully examined before extending our findings to large-scale river systems. Specifically, while a 1-D filter with spatially uncorrelated model representation error may be appropriate for small-basin correction, ignoring the spatial correlation structure of errors could potentially have a more profound impact on the correction performance at large river outlets where streamflow originates from runoff from a large number of grid cells. Multiple studies have investigated the effects of spatial error patterns in hydrologic data assimilation. For example, Reichle and Koster (2003) investigated the impact of spatial error correlation in the model SM states on its assimilation performance; Gruber et al. (2015) examined the impact of a 2-D filter with spatially auto-correlated error versus a 1-D filter on SM updating quality; Pan et al. (2009) and Pan and Wood (2009; 2010) evaluated the surface SM assimilation performance with VIC by comparing a 1-D filter, a 2-D filter and a multiscale autoregressive filtering approach, as well as considering spatial and temporal structure of precipitation error. ~~Given the above considerations, we may be approaching a point of diminishing returns for applying data assimilation techniques that are aimed solely at reducing random error sources in streamflow simulations. This insight provides few recommendations for future research:~~

~~1) More sophisticated data assimilation techniques aimed solely at random error sources are unlikely to substantially reduce streamflow error further, since random errors sometimes account for only a relatively small portion of the total error;~~

~~2)~~However, all these studies focused exclusively on the performance of SM simulations. Direct assessment of the impact of spatial error patterns on the routed streamflow results is needed, especially from a probabilistic perspective since the ignorance of spatial error patterns (and therefore their potential to mutually cancel as runoff is routed through a river network) will lead to an incorrect ensemble representation of streamflow uncertainty.

Another factor that may have limited the dual correction performance, particularly the state updating scheme, is the rescaling of the SMAP retrievals to the VIC top-layer SM regime. Matching a satellite-observed SM product with that represented in a land surface model (LSM) is a necessary pre-processing step in a data assimilation system; however, it has the well-known limitation of neglecting potential bias-correction information contained in the satellite-observed product. While this problem is well-discussed in the literature (see, e.g., Yilmaz et al., 2013; Kumar et al., 2015; Nearing et al., 2018), no robust solutions currently exist. Ideally, the physical source of remote sensing and modelling biases could be isolated and addressed. However, this is very difficult to do in practice. For instance, although SMAP is typically described as measuring the top ~ 5 cm of SM, the actual vertical support depth is unclear and varies nonlinearly as a function of SM and vegetation water content. In addition, the relationship between the top-layer depth and its SM dynamics in an LSM is complex and driven by multiple poorly known model parameters (although, Shellito et al. (2018) found that changing the top-layer depth from 10 cm to 5 cm in the Noah LSM did not significantly affect surface SM dynamics). Therefore, like other existing SM data assimilation applications, we are forced to resort to an ad hoc solution where satellite-based observations are rescaled to match the climatological characteristics of equivalent model products.

~~Instead, approaches that reduce systematic errors in streamflow simulation are needed. To date this is still a challenging task in large-scale hydrologic modeling, since calibration is difficult to perform with limited streamflow data and a large number of distributed parameters. With the availability of the near-global and distributed satellite products such as SMAP and IMERG, more creative methods need to be developed to extract useful information from the large volume of remote sensing observations. For example, characteristics of SM dynamics and its response to rainfall can be directly extracted from the datasets themselves, which can~~

~~potentially inform hydrologic model representation. These areas of research are less studied but have the potential to improve hydrologic modeling beyond correcting random errors;~~

~~3) It is worthwhile to continue to develop future generation of higher-quality, near-real-time rainfall products, since rainfall plays a dominant role in streamflow simulations and its error is not easily and substantially reduced by the current correction methods that use SM measurement information.~~

5. Conclusion

In this paper, we applied a dual state/rainfall correction data assimilation system in the Arkansas-Red River basin. Built upon the dual system developed in past studies, we have made several methodological advances. First, we implemented the dual correction system with a more ~~complexed~~complex, semi-distributed land surface model~~, the~~ (VIC~~ model,~~) and applied it in a regional-scale basin. Second, the latest satellite products, the SMAP SM product and the IMERG rainfall product, were incorporated into the system. Third, the existing dual correction algorithm was extended to maximize the use of information contained in the more accurate, and temporally ~~finer~~more frequent, satellite data products~~, and also~~. Fourth, the SMART approach has been modified to produce an ensemble streamflow product~~. Fourth~~ to generate probabilistic estimates. Fifth, we confirmed via a formal synthetic experiment that error cross-correlation that potentially exists in the dual correction system does not cause noticeable degradation of streamflow improvement~~,~~ and the dual correction scheme applied here is optimal.

Our results show that, overall, the SMART algorithm is able to correct IMERG rainfall slightly to moderately, and the correction is more effective during larger rainfall events and at daily to multi-daily time scales. The ensemble produced by the correction scheme represents the rainfall uncertainty relatively well. However, the rainfall correction we achieved is generally smaller than found by previous studies, mainly due to improved quality of the baseline satellite rainfall product over time. In addition, although SMAP arguably also has higher quality than older remotely-sensed SM products, its quality remains relatively low in dense-biomass regions, resulting in reduced rainfall correction via SMART.

Combined with analogous improvement in pre-storm SM states, the relatively small rainfall correction is propagated into VIC and generally results in improved streamflow estimates. However, the improvements found are relatively small and vary greatly between sub-basins. Due to its deleterious impact on SMAP retrieval uncertainty, small improvement is found in sub-basins containing dense biomass. Furthermore, the dual data assimilation system is only designed to correct zero-mean random errors and not systematic errors or bias. However, systematic errors can account for a substantial fraction of the total streamflow error. This results in relatively modest streamflow correction via the Kalman-filter-based correction system and the significant underestimation of uncertainty in VIC streamflow estimates.

Given the above findings, we provide the following recommendations for future research:

1) Higher-quality SM retrievals are necessary to push the current limit of rainfall correction (and, consequently, streamflow correction) especially in areas of dense vegetation.

2) However, even with better SM data quality, data assimilation techniques aimed solely at random error sources are unlikely to substantially reduce streamflow errors in many sub-basins, since random errors often account for only a relatively small portion of the total error. Instead, approaches that reduce systematic errors in streamflow simulation are needed. ~~Our results show that, overall, IMERG rainfall and streamflow are improved to some extent but not substantially via dual correction. For rainfall, the improvement is primarily from the correction of larger events via SMART, while smaller events are slightly degraded. Rainfall correction is more effective at daily to multi-daily time scales than at a 3-hourly scale. The ensemble produced by the correction scheme represents the rainfall uncertainty relatively well at daily to multi-daily scale. For streamflow, the dual correction reduces the random errors in simulated streamflow across the 8 test sub-basins, ranging from near zero improvement to moderate error reduction. Sub-basins with relatively poorer open-loop streamflow simulations, due mainly to poor IMERG rainfall forcing quality, exhibit relatively larger correction, and the correction is mainly contributed by the SMART rainfall correction scheme. Sub-basins with relatively better IMERG and open-loop streamflow show less relative correction, and the correction is attributable more to state updating. The streamflow ensemble produced by the dual correction system largely underestimates error uncertainty, because the system accounts only for the~~

Formatted: Indent: First line: 0.5"

~~random error components and not systematic error (resulting, e.g., from incorrect model structure or parameterization). Finally, we demonstrated that model parameterization errors that commonly exist in large-scale distributed models in general does not degrade (and sometimes actually benefits) the relative added value of the dual correction scheme.~~

~~These findings suggest that we are approaching a point of diminishing returns for SM data assimilation techniques aimed solely at the reduction of random errors in simulated streamflow. More sophisticated SM data assimilation techniques may lead to additional marginal improvement, but more substantial streamflow reduction likely require future research efforts on reducing systematic modeling errors via, e.g., innovative ways of achieving better model representation as well as obtaining higher-quality satellite rainfall products.~~

To date, this is still a challenging task in large-scale hydrologic modeling, since robust calibration is difficult to achieve with limited streamflow data and many distributed parameters. With the availability of the near-global and distributed satellite products such as SMAP and IMERG, more creative methods are needed to extract useful information from the large volume of remote sensing observations. For example, the characteristics of SM dynamics and its response to rainfall can be directly extracted from the datasets themselves, which can potentially inform hydrologic model representation. These new areas of research have the potential to improve hydrologic modeling beyond the correction of random errors.

Code availability

The VIC model used in the study can be found at https://github.com/UW-Hydro/VIC. Specifically, we used VIC version 5.0.1 (doi:10.5281/zenodo.267178) with a modification to the calculation of drainage between soil layers (https://github.com/UW-Hydro/VIC/releases/tag/Mao_etal_stateDA_May2018). The DA code used in this study is available at https://github.com/UW-Hydro/dual_DA_SMAP.

Author contribution

All co-authors designed the experiments. Yixin Mao developed the system code and carried out the experiments. Wade T. Crow and Bart Nijssen supervised the study. Yixin Mao prepared the manuscript with contributions from all co-authors.

Competing interests

The authors declare that they have no conflict of interest.

Acknowledgements

This work was supported in part by NASA Terrestrial Hydrology Program Award NNX16AC50G to the University of Washington and NASA Terrestrial Hydrology Program Award 13-THP13-0022 to the United States Department of Agriculture, Agricultural Research Service. Yixin Mao also received a Pathfinder Fellowship by CUAHSI with support from the National Science Foundation (NSF) Cooperative Agreement No. EAR-1338606. We would also like to thank Andrew Wood from NCAR for help on calibration.

References

Alvarez-Garreton, C., Ryu, D., Western, A. W., Crow, W. T., and Robertson, D. E.: The impacts of assimilating satellite soil moisture into a rainfall-runoff model in a semi-arid catchment, J. Hydrol., 519, 2763-2774, doi:10.1016/j.jhydrol.2014.07.041, 2014.

Alvarez-Garreton, C., Ryu, D., Western, A. W., Crow, W. T., Su, C.-H., and Robertson, D. R.: Dual assimilation of satellite soil moisture to improve streamflow prediction in data-scarce catchments, Water Resour. Res., 52(7), 5357-5375, doi:10.1002/2015WR018429, 2016.

Aubert, D., Loumagne, C., and Oudin, L.: Sequential assimilation of soil moisture and streamflow data in a conceptual rainfall-runoff model, J. Hydrol., 280(1-4), 145-161, doi:10.1016/S0022-1694(03)00229-4, 2003.

Bolten, J. D. and Crow, W. T.: Improved prediction of quasi-global vegetation conditions using remotely-sensed surface soil moisture. Geophys. Res. Lett.. 39, L19406, doi:10.1029/2012GL053470, 2012.

Brocca, L., Melone, F., Moramarco, T., Wagner, W., Naeimi, V., Bartalis, Z., and Hasenauer, S.: Improving runoff prediction through the assimilation of the ASCAT soil moisture product, Hydrol. Earth Syst. Sci., 14, 1881-1893, doi:10.5194/hess-14-1881-2010, 2010.

Brocca, L., Moramarco, T., Melone, F., Wagner, W., Hasenauer, S., and Hahn, S.: Assimilation of surface-and root-zone ASCAT soil moisture products into rainfall–runoff modeling, IEEE Trans. Geosci. Remote Sens., 50(7), 2542-2555, doi:10.1109/TGRS.2011.2177468, 2012.

Brocca, L., Moramarco, T., Melone, F., and Wagner, W.: A new method for rainfall estimation through soil moisture observations, Geophys. Res. Lett., 40, 853–858, doi:10.1002/grl.50173, 2013.

Brocca, L., Ciabatta, L., Massari, C., Moramarco, T., Hahn, S., Hasenauer, S., Kidd, R., Dorigo, W., Wagner, W., and Levizzani, V.: Soil as a natural rain gauge: Estimating global rainfall from satellite soil moisture data, J. Geophys. Res. Atmos., 119, 5128–5141, doi:10.1002/2014JD021489, 2014.

Brocca, L., Pellarin, T., Crow, W. T., Ciabatta, L., Massari, C., Ryu, D., Su, C.-H., Rüdiger, C., and Kerr, Y.: Rainfall estimation by inverting SMOS soil moisture estimates: A comparison of different methods over Australia, J. Geophys. Res. Atmos., 121, 12,062–12,079, doi:10.1002/2016JD025382, 2016.

Chan, S. et al.: Development and validation of the SMAP enhanced passive soil moisture product, Geoscience and Remote Sensing Symposium (IGARSS), 2017 IEEE International, doi:10.1109/IGARSS.2017.8127512, 2017.

Chen F., Crow, W. T., and Holmes, T. R. H.: Improving long-term, retrospective precipitation datasets using satellite-based surface soil moisture retrievals and the Soil Moisture Analysis Rainfall Tool, J. Appl. Remote Sens., 6(1), 063604, doi:10.1117/1.JRS.6.063604, 2012.

Chen, F., Crow, W. T., and Ryu, D.: Dual forcing and state correction via soil moisture assimilation for improved rainfall–runoff modeling, J. Hydrometeorol., 15(5), 1832–1848, doi:10.1175/JHM-D-14-0002.1, 2014.

Colliander, A. et al.: Validation of SMAP surface soil moisture products with core validation sites, Remote Sens. Environ., 191, 215-231, doi:10.1016/j.rse.2017.01.021, 2017.

Crow, W. T., and Bolten, J. D.: Estimating precipitation errors using spaceborne surface soil moisture retrievals, Geophys. Res. Lett., 34, L08403, doi:10.1029/2007GL029450, 2007.

Crow, W. T., and Ryu, D.: A new data assimilation approach for improving ~~hydrologic~~runoff prediction using remotely-sensed soil moisture retrievals, Hydrol. Earth Syst. Sci., 12(1-16), doi:10.5194/hess-13-1-2009, 2009.

Crow W. T., Huffman, G. J., Bindlish, R., and Jackson, T. J.: Improving satellite-based rainfall accumulation estimates using spaceborne surface soil moisture retrievals, J. Hydrometeorol., 10, 199-212, doi:10.1175/2008JHM986.1, 2009.

Crow, W. T., and van den Berg, M. J.: An improved approach for estimating observation and model error parameters for soil moisture data assimilation, Water Resour. Res., 46, W12519, doi:.10.1029/2010WR009402. 2010.

Crow, W. T., van den Berg, M. J., Huffman, G. J., and Pellarin, T.: Correcting rainfall using satellite-based surface soil moisture retrievals: The Soil Moisture Analysis Rainfall Tool (SMART), Water Resour. Res., 47, W08521, doi:10.1029/ 2011WR010576, 2011.

Crow, W. T., Chen, F., Reichle, R. H., and Liu, Q.: L band microwave remote sensing and land data assimilation improve the representation of prestorm soil moisture conditions for hydrologic forecasting, Geophys. Res. Lett., 44, 5495-5503, doi:10.1002/2017GL073642, 2017.

De Lannoy, G. J. M., Houser, P. R., Pauwels, V. R. N., and Verhoest, N. E. C.: Assessment of model uncertainty for soil moisture through ensemble verification, J. Geophys. Res., 111, D10101, doi:10.1029/2005JD006367, 2006.

Dong, J., Crow, W. T., Reichle, R., Liu, Q., Lei, F. and Cosh, M.: A global assessment of added value in the SMAP Level 4 soil moisture product relative to its baseline land surface model. Geophys. Res. Lett., 46:6604-6613, doi:10.1029/2019GL083398, 2019.

Formatted: Strong

Formatted: Font: Times New Roman, 12 pt, Font color: Custom Color(RGB(28,29,30)), Pattern: Clear (White)

Entekhabi et al.: The Soil Moisture Active and Passive (SMAP) Mission, Proceedings of the IEEE, 98(5), 704-716, doi:10.1109/JPROC.2010.2043918, 2010.

Francois, C., Quesney, A., and Ottle, C.: Sequential assimilation of ERS-1 SAR data into a coupled land surface-hydrological model using an extended Kalman filter, J. Hydrometeorol., 4(2), 473-487, doi:10.1175/1525-7541(2003)4<473:SAOESD>2.0.CO;2, 2003.

Freeze, R. A., and Harlan, R. L.: Blueprint for a physically-based, digitally-simulated hydrologic response model, J. Hydrol., 9(3), 237-258, doi:10.1016/0022-1694(69)90020-1, 1969.

Gebregiorgis, A. S., Kirstetter, P.-E., Hong, Y. E., Gourley, J. J., Huffman, G. J. Petersen, W. A., Xue, X., and Schwaller, M. R.: To what extent is the day 1 GPM IMERG satellite precipitation estimate improved as compared to TRMM TMPA-RT?, J. Geophys. Res. Atmos., 123, 1694–1707, doi:10.1002/2017JD027606, 2018.

Gruber, A., Crow, W. T., Dorigo, W., and Wagner, W.: The potential of 2D Kalman filtering for soil moisture data assimilation, Remote Sens. Environ., 171, 137-148, doi:10.1016/j.rse.2015.10.019, 2015.

Gupta, H. V., Kling, H. Kling, Yilmaz, K. K., and Martinez, G. F.: Decomposition of the mean squared error and NSE performance criteria: Implications for improving hydrological modelling, J. Hydrol., 377, 80-91, doi:10.1016/j.jhydrol.2009.08.003, 2009.

Hamman, J., Nijssen, B., Roberts, A., Craig, A., Maslowski, W., and Osinski, R.: The coastal streamflow flux in the Regional Arctic System Model, J. Geophys. Res., 122(3), 1683-1701, doi:10.1002/2016JC012323, 2017.

Hamman, J. J., Nijssen, B., Bohn, T. J., Gergel, D. R., and Mao, Y.: The Variable Infiltration Capacity Model, Version 5 (VIC-5): Infrastructure improvements for new applications and reproducibility, Geosci. Model Dev., 11, 3481-3496, doi:10.5194/gmd-11-3481-2018, 2018.

Hou, A. Y., Kakar, R. K., Neeck, S., Azarbarzin, A. A., Kummerow, C. D., Kojima, M., Oki, R., Nakamura, K., and Iguchi, T.: The Global Precipitation Measurement mission, Bull. Amer. Meteor. Soc., 95(5), 701-722, doi:10.1175/BAMS-D-13-00164.1, 2014.

Huffman, G. J., Bolvin, D. T., and Nelkin, E. J.: Integrated Multi-Satellite Retrievals for GPM (IMERG) Technical Documentation. Tech. Doc., NASA GSFC, available online at https://docserver.gesdisc.eosdis.nasa.gov/public/project/GPM/IMERG_doc.05.pdf, 2015.

Huffman, G. J., Stocker, E. F., Bolvin, D. T., and Nelkin, E. J.: last updated 2018: IMERG L3 Early Run Data Sets. NASA/GSFC, Greenbelt, MD, USA, accessed 2018-08-29, https://gpm1.gesdisc.eosdis.nasa.gov/opendap/hyrax/GPM_L3/GPM_3IMERGHHL.05/, 2018.

Koster, R. D., Brocca, L., Crow, W. T., Burgin, M. S., and De Lannoy, G. J. M.: Precipitation estimation using L-band and C-band soil moisture retrievals, Water Resour. Res., 52, 7213–7225, doi:10.1002/2016WR019024, 2016.

Kumar, S. V., Peters-Lidard, C. D., Santanello, J. A., Reichle, R. H., Draper, C. S., Koster, R. D., Nearing, G., and Jasinski, M. F.: Evaluating the utility of satellite soil moisture retrievals over irrigated areas and the ability of land data assimilation methods to correct for unmodeled processes, Hydrol. Earth Syst. Sci., 19, 4463–4478, doi:10.5194/hess-19-4463-2015, 2015.

Liang, X., Lettenmaier, D. P., Wood, E. F., and Burges, S. J.: A simple hydrologically based model of land surface water and energy fluxes for general circulation models, J. Geophys. Res., 99(D7), 14415-14428, doi:10.1029/94JD00483, 1994.

Lievens, H., et al.: SMOS soil moisture assimilation for improved hydrologic simulation in the Murray Darling Basin, Australia, Remote Sens. Environ., 168, 146-162, doi:10.1016/j.rse.2015.06.025, 2015.

Lievens, H., De Lannoy, G. J. M., Al Bitar, A., Drusch, M., Dumedah, G., Hendricks Franssen, H.-J., Kerr, Y. H., Tomer, S. K., Martens, B., Merlin, O., Pan, M., Roundy, J. K., Vereecken, H., and Walker, J. P.: Assimilation of SMOS soil moisture and brightness temperature products into a land surface model, Remote Sens. Environ., 180, 292-304, doi:10.1016/j.rse.2015.10.033, 2016.

Lohmann, D., Nolte-Holube, R., and Raschke, E.: A large-scale horizontal routing model to be coupled to land surface parametrization schemes, Tellus, 48(A), 708-721, doi:10.1034/j.1600-0870.1996.t01-3-00009.x, 1996.

Lohmann, D., Raschke, E., Nijssen, B., and Lettenmaier, D. P.: Regional scale hydrology: I. Formulation of the VIC-2L model coupled to a routing model, Hydrol. Sci. J., 43(1), 131-141, doi:10.1080/02626669809492107, 1998.

Mao Y., Crow, W. T., and Nijssen, B.: A framework for diagnosing factors degrading the streamflow performance of a soil moisture data assimilation system, J. Hydrometeorol., 20(1), 79-97, doi:10.1175/JHM-D-18-0115.1, 2019.

Massari, C., Brocca, L., Tarpanelli, A., and Moramarco, T.: Data Assimilation of Satellite Soil Moisture into Rainfall-Runoff Modelling: A Complex Recipe?, Remote Sens., 7, 11403-11433, doi:10.3390/rs70911403, 2015.

Massari, C., Camici, S., Ciabatta, L., and Brocca, L.: Exploiting satellite-based surface soil moisture for flood forecasting in the Mediterranean area: State update versus rainfall correction, Remote Sens., 10, 292, doi:10.3390/rs10020292, 2018.

Maurer, E. P., Wood, A.W., Adam, J. C., Lettenmaier, D. P., and Nijssen, B.: A long-term hydrologically-based data set of land surface fluxes and states for the conterminous United States, J. Clim., 15(22), 3237-3251, doi:10.1175/1520-0442(2002)015<3237:ALTHBD>2.0.CO;2, 2002.

Mehra, R. K.: On-line identification of linear dynamic systems with applications to Kalman filtering, IEEE Trans. Autom. Control., 16(1), 12-21, doi:10.1109/TAC.1971.1099621, 1971.

Nearing, G., Yatheendradas, S., Crow, W.T., Chen, F. and Zhan, X: The efficiency of data assimilation, Water Resour. Res., 54:6374–6392, doi:10.1029/2017WR020991, 2018.

O'Neill, P. E., Chan, S., Njoku, E. G., Jackson, T., and Bindlish, R.: SMAP L3 Radiometer Global Daily 36 km EASE-Grid Soil Moisture, Version 4, Boulder, Colorado USA, NASA National Snow and Ice Data Center Distributed Active Archive Center, Accessed 2018-01-18, doi:10.5067/OBBHQ5W22HME, 2016.

Pan, M., and Wood, E. F.: A multiscale ensemble filtering system for hydrologic data assimilation. Part II: Application to land surface modeling with satellite rainfall forcing, J. Hydrometeorol., 10, 1493-1506, doi:10.1175/2009JHM1155.1, 2009.

Pan, M., and Wood, E. F.: Impact of accuracy, spatial availability, and revisit time of satellite-derived surface soil moisture in a multiscale ensemble data assimilation system, IEEE J. Sel. Topics Appl. Earth Observ. Remote Sens., 3 (1), 49-56, doi:10.1109/JSTARS.2010.2040585, 2010.

Pan, M., Wood, E. F., McLaughlin, D. B., and Entekhabi, D.: A multiscale ensemble filtering system for hydrologic data assimilation. Part I: Implementation and synthetic experiment, J. Hydrometeorol., 10, 794-806, doi:0.1175/2009JHM1088.1, 2009.

Qing, L., Reichle, R., Bindlish, R., Cosh, M. H., Crow, W.T., de Jeu, R., de Lannoy, G., Huffman, G. J. and Jackson, T. J.: The contributions of precipitation and soil moisture observations to the skill of soil moisture estimates in a land data assimilation system, J. Hydrometeorol.. 12(5):750-765, doi:10.1175/JHM-D-10-05000.1, 2011.

Reichle, R. H., and Koster, R. D.: Assessing the impact of horizontal error correlations in background fields on soil moisture estimation, J. Hydrometeorol., 4 (6), 1229-1242, doi:10.1175/1525-7541(2003)004<1229:ATIOHE>2.0.CO;2, 2003.

Reichle, R.H., Crow, W. T., Koster, R. D., Sharif, H. and Mahanama, S.: Contribution of soil moisture retrievals to land data assimilation products, Geophys. Res. Lett., 35, L01404, doi:10.1029/2007GL031986, 2008.

Shellito, P. J., Small, E. E., and Livneh B.: Controls on surface soil drying rates observed by SMAP and simulated by the Noah land surface model, Hydrol. Earth Syst. Sci., 22, 1649-1663, doi:10.5194/hess-22-1649-2018, 2018.

Talagrand, O., Vautard, R., and Strauss, B.: Evaluation of probabilistic prediction systems, technical report, Eur. Cent. for Medium-Range Weather Forecast., Reading, UK, 1997.

United States Geological Survey (USGS): USGS Surface-water daily data for the nation, available at https://waterdata.usgs.gov/nwis/dv/?referred_module=sw, 2018.

Wanders, N., Karssenberg, D., De Roo, A., De Jong, S. M., and Bierkens, M. F. P.: The suitability of remotely sensed soil moisture for improving operational flood forecasting, Hydrol. Earth Syst. Sci., 18(6), 2343-2357, doi:10.5194/hess-18-2343-2014, 2014.

Western, A. W., Grayson, R. B., and Blöschl, G., Scaling of soil moisture: a hydrologic perspective, Annu. Rev. Earth Planet. Sci., 30(1), 149-180, doi:10.1146/annurev.earth.30.091201.140434, 2002.

Wilks, D. S.: Statistical methods in the atmospheric sciences (3rd edition), Elsevier/Academic Press, Amsterdam; Boston, 2011.

Formatted: Space Before: Auto, After: Auto

Xia, Y. et al., NCEP/EMC: NLDAS Primary Forcing Data L4 Hourly 0.125 x 0.125 degree V002, Edited by David Mocko, NASA/GSFC/HSL, Greenbelt, Maryland, USA, Goddard Earth Sciences Data and Information Services Center (GES DISC), accessed 2018-02-27, doi:10.5067/6J5LHHOHZHN4, 2009.

Xia, Y., et al.: Continental-scale water and energy flux analysis and validation for the North American LandData Assimilation System project phase 2 (NLDAS-2): 1. Intercomparison and application of model products, J. Geophys. Res.,117, D03109, doi:10.1029/2011JD016048.1, 2012.

Yapo, P. O., Gupta, H. V., and Sorooshian, S.: Multi-objective global optimization for hydrologic models, J. Hydrol. 2014, 83-97, doi:10.1016/S0022-1694(97)00107-8, 1998.

Yilmaz, M.T. and Crow, W.T: The optimality of potential rescaling approaches in land data assimilation, J. Hydrometeorol., 14:650-660, doi:10.1175/JHMD12052.1, 2013.

Table 1. List of USGS streamflow sites used for verification.

Basin number	USGS station no.	USGS station name	Short name
1	07144200	Little Arkansas River at Valley Center, KS	L Arkansas
2	07144780	Ninnescah River AB Cheney Re, KS	Ninnescah
3	07147800	Walnut River at Winfield, KS	Walnut
4	07152000	Chikaskia River near Blackwell, OK	Chikaskia
5	07177500	Bird Creek Near Sperry, OK	Bird
6	07186000	Spring River near Wace, MO	Spring
7	07196500	Illinois River near Tahlequah, OK	Illinois
8	07243500	Deep Fork near Beggs, OK	Deep

Table 2. ~~Review of SMART rainfall correction results in literature along with the results in this study.~~

~~Literature~~	~~Baseline rainfall product~~	~~Benchmark rainfall product~~	~~SM product~~	~~Domain~~	~~Accumulation period~~	~~Baseline correlation *r*~~	~~*r* improvement~~	~~Baseline RMSE (mm)~~	~~PER~~
~~Crow et al. (2009)~~	~~TRMM 3B40RT~~	~~CPC rain gauge analysis~~	~~AMSR-E~~	~~Southern Great Plain~~ ~~CONUS~~	~~3-day~~ ~~3-day~~	~~~ 0.5~~ ~~~ 0.55~~	~~~ + 0.2~~ ~~~ + 0.05~~	~~13.0~~ ~~11.8~~	~~~ 30%~~ ~~~ 15%~~
~~Crow et al. (2011)~~	~~TRMM 3B40RT~~	~~CPC rain gauge analysis~~	~~AMSR-E~~	~~CONUS~~	~~3-day~~	~~~ 0.55~~	~~~ + 0.1~~	~~13.1~~	~~~ 20%~~
~~Chen et al. (2012)~~	~~Princeton Global Forcing Dataset~~	~~CPC rain gauge analysis~~	~~SMMR, SMM/I, ERS~~	~~Global~~	~~10-day~~	~~~ 0.35~~	~~~ + 0.15~~	~~-~~	~~-~~
~~Brocca et al. (2016)~~	~~TRMM 3B42RT~~	~~AWAP rain gauge product~~	~~SMOS~~	~~Australia~~	~~1-day~~ ~~5-day~~	~~0.62~~ ~~0.71~~	~~+0.01~~ ~~+0.05~~	~~5.6~~ ~~14.0~~	~~7%~~ ~~14%~~
~~This study~~	~~IMERG Early Run~~	~~NLDAS-2~~	~~SMAP L3 Passive~~	~~Arkansas-Red~~	~~1-day~~ ~~3-day~~	~~0.80~~ ~~0.82~~	~~+0.02~~ ~~+0.02~~	~~6.1~~ ~~11.0~~	~~8%~~ ~~8%~~

~~**Table 3.**~~ Daily streamflow results from the dual correction system for the ~~8~~eight USGS sub-basins shown in Fig. 1. In addition to the deterministic KGE improvement, PER and probabilistic NENSK results from the dual system ("*dual*" columns), the table also lists the open-loop streamflow KGE ("*open-loop KGE*" column), KGE improvement and PER as a result of state update or rainfall correction scheme alone ("*state update only*" and "*rainfall correction only*" columns, respectively), and KGE improvement and PER when forced by the NLDAS-2 benchmark precipitation without state update ("*NLDAS-2 forced*" column).

	Open-loop KGE	KGE improvement				PER				NENSK
		Dual	State update only	Rainfall correction only	NLDAS2-forced	Dual	State update only	Rainfall correction only	NLDAS2-forced	Dual
L Arkansas	-0.12	+0.17	+0.23	-0.01	+0.57	7.3%	10.8%	1.2%	40.0%	1.98
Ninnescah	0.25	+0.15	+0.06	+0.16	+0.20	14.0%	5.5%	13.7%	30.4%	0.35
Walnut	0.54	-0.02	-0.03	+0.03	-0.23	5.8%	5.7%	2.8%	23.3%	2.70
Chikaskia	0.67	+0.07	+0.05	+0.02	-0.45	15.0%	11.1%	6.6%	2.2%	1.96
Bird	-1.49	+0.95	+0.58	+0.63	+0.95	33.5%	17.0%	25.8%	68.9%	2.01
Spring	-3.64	+0.83	+0.65	+0.33	+3.93	13.2%	8.7%	7.0%	83.4%	13.11
Illinois	-1.91	+0.50	+0.36	+0.26	+2.72	17.6%	7.4%	12.9%	81.8%	13.78
Deep	-0.77	+0.49	+0.39	+0.37	+1.55	20.8%	13.1%	21.2%	68.3%	2.34

Table 3. Review of SMART rainfall correction results in literature along with the results in this study.

Literature	Baseline rainfall product	Benchmark rainfall product	SM product	Domain	Accumulation period	Baseline correlation *r*	*r* improvement	Baseline RMSE (mm)	PER
Crow et al. (2009)	TRMM 3B40RT	CPC rain gauge analysis	AMSR-E	Southern Great Plain CONUS	3-day 3-day	~ 0.5 ~ 0.55	~ + 0.2 ~ + 0.05	13.0 11.8	~ 30% ~ 15%
Crow et al. (2011)	TRMM 3B40RT	CPC rain gauge analysis	AMSR-E	CONUS	3-day	~ 0.55	~ + 0.1	13.1	~ 20%
Chen et al. (2012)	Princeton Global Forcing Dataset	CPC rain gauge analysis	SMMR, SMM/I, ERS	Global	10-day	~ 0.35	~ + 0.15	-	-
Brocca et al. (2016)	TRMM 3B42RT	AWAP rain gauge product	SMOS	Australia	1-day 5-day	0.62 0.71	+0.01 +0.05	5.6 14.0	7% 14%
This study	IMERG Early Run	NLDAS-2	SMAP L3 Passive	Arkansas-Red	1-day 3-day	0.80 0.82	+0.02 +0.02	6.1 11.0	8% 8%

998

Supplemental Material

Style Definition: Comment Text

Dual state/rainfall correction via soil moisture assimilation for improved streamflow simulation: Evaluation of a large-scale implementation with SMAP satellite data

Yixin Mao[1], Wade T. Crow[2] and Bart Nijssen[1]

1: Department of Civil and Environmental Engineering, University of Washington, Seattle, WA

2: Hydrology and Remote Sensing Laboratory, Agricultural Research Service, USDA, Beltsville, MD

Corresponding author: Bart Nijssen (nijssen@uw.edu)

S1. The ensemble Kalman smoother (EnKS) version of the Soil Moisture Analysis Rainfall Tool (SMART)

The Soil Moisture Analysis Rainfall Tool (SMART) is a rainfall correction scheme developed and updated by Crow et al. (2009; 2011) and Chen et al. (2012). It is based on sequential assimilation of soil moisture (SM) measurements into a simple Antecedent Precipitation Index (API) model to obtain SM increments~~, and~~. It then linearly relates these increments to rainfall accumulation errors. In the study we extended the ensemble Kalman filter (EnKF) version of SMART developed by Crow et al. (2011) to an ensemble Kalman smoother (EnKS) version with probabilistic rainfall estimates.

Following Crow et al. (2009; 2011), the API model is used to capture the response of moisture storage (represented by the *API* state) to rainfall input:

$$API_t = \gamma API_{t-1} + P_t \qquad \text{(S1)}$$

where t is a ~~timestep~~time step index; P is the original uncorrected precipitation observation [mm] and γ is a loss coefficient (dimensionless) that accounts for storage loss through evaporation, drainage, etc. In the ensemble version of SMART (Crow et al., 2011), Eq. (S1) is converted to:

$$API_t^{(j)} = \gamma API_{t-1}^{(j)} + \eta_t^{(j)} P_t + \omega_t^{(j)} \qquad \text{(S2)}$$

where the superscript *(j)* denotes the *j*th ensemble member; η is multiplicative noise with mean 1 added to the observed precipitation to represent random precipitation forcing error; and ω is zero-mean Gaussian noise to represent random API model structure and parameterization error. The API state can be related directly to SM content via rescaling (Crow et al., 2009). The rescaled SM measurement, θ, can therefore be assimilated to update the *API* states via the standard EnKS technique both at the measurement ~~timestep~~time step and during the data gap before the measurement ~~timestep~~time step. Mathematically, if two adjacent measurements come in at time k and time m with $m - k \geq 1$, then the measurement at time m is used to calculate the gain K and API increment δ for each ~~timestep~~time step i at ~~timestep~~time step m as well as during the gap (i.e., $k < i \leq m$):

$$K_i = \frac{T_{im}}{T_m + R_m} \tag{S3}$$

and

Formatted: Space After: 8 pt

$$\delta_i^{(j)} = API_i^{+(j)} - API_i^{-(j)} = K_i \cdot (\theta_m + \kappa_m^{(j)} - API_m^{-(j)}) \tag{S4}$$

where K is the Kalman gain; T_{im} is the covariance matrix between *API* states at time i and m; R is the measurement error variance for the rescaled SM measurements; the superscript *(j)* denotes the *j*th ensemble member; the superscripts "-" and "+" denote *API* states before and after an update, respectively; and κ is zero-mean Gaussian noise added to represent the random SM measurement error. T_{im} is calculated as:

$$T_{im} = \frac{1}{M-1}\sum_{j=1}^{M}(API_i^{-(j)} - \overline{API}_i^{-}) \cdot (API_m^{-(j)} - \overline{API}_m^{-}) \tag{S5}$$

where M is the ensemble size; $\overline{API}_t^{-}$ is the ensemble-mean *API* states before update.

The SMART algorithm then uses ensemble-mean *API* increment δ to estimate the rainfall correction amount via a simple linear relation. We extended this relation to produce an ensemble of corrected rainfall time series (instead of the single rainfall estimates in past studies) where each ensemble member of the perturbed rainfall time series is corrected by the corresponding member of δ.:

Formatted: Space After: 8 pt

$$[P_{corr}^{(j)}]_l = [\eta^{(j)} P^{(j)}]_l + \lambda[\delta^{(j)}]_l \quad \text{(S6)}$$

where "[ ]" denotes temporally aggregated P or δ (in the SMART study in this paper, this window was set to the 3-hour native SMART ~~timestep~~time step without aggregation); l is the new time index for the aggregated windows; and λ is a scaling factor that can either be calibrated or set to a prescribed constant. Finally, negative P_{corr} resulted from Eq. (S6) are reset to zero, and the final corrected precipitation time series is (multiplicatively) rescaled to be unbiased over the entire simulation period toward the original precipitation observation time series.

S2. Mathematical details of ensemble Kalman filter (EnKF) in the state update scheme

The ensemble Kalman filter (EnKF) method is a commonly used data assimilation (DA) techniques in hydrology. The EnKF technique applied in this study directly follows Mao et al. (2019). Below will briefly review its mathematical details.

The EnKF algorithm was applied to each SMAP pixel individually. The EnKF method is based on a propagation model and a measurement model:

$$x_{k+1} = f(x_k, u_k) + \omega_k \quad \text{(S7)}$$

$$\tilde{y}_k = Hx_k + v \quad \text{(S8)}$$

where subscript k is a discrete time index; x is a column vector of model states to update (the column vector length is the total number of state variables to update), which, in our application, is top-layer VIC-simulated SM estimates in every finer-resolution VIC grid cell that is associated with a SMAP pixel; u is model meteorological forcing, in our context rainfall; $f()$ is a land surface model that propagates states to the next time step, in our context the VIC model; ω lumps together modeling errors during propagation from various sources including forcing data error, model structure error and parameterization error; $\tilde{y}$ is measurement data, in our context surface SM measurements, i.e., $\tilde{y} = SM_1^{obs}$ where SM_1^{obs} is the SMAP observation at its native coarser resolution; H is an observation operator that relates model states x to measurements $\tilde{y}$, in our contex the areal-averaged first-layer SM state from the multiple VIC grid cells; and v is random measurement error.

In a standard EnKF, an ensemble size of *N* model replicates is propagated and updated sequentially over time in the following way:

1) An ensemble of initial model states is first generated by perturbing the initial deterministic model states (all three VIC SM layers in our context) to represent initial state error;

2) For each ensemble member, the land surface model is run until the next measurement time with perturbed meteorological forcing to represent forcing error. Model states are directly perturbed as well (again, all three VIC SM layers) to represent random errors from model structure and parameterization;

3) Once an observation time is reached, the Kalman gain *K* is calculated as:

$$K_k = P_k H^T \cdot (HP_k H^T + R)^{-1} \tag{S9}$$

Field Code Changed

where *R* is the measurement error variance, and the forecast state error covariance matrix P_k is estimated by sampling across the propagated ensemble states:

$$P_k = \frac{1}{N-1}\sum_{j=1}^{N}(\hat{x}_k^{-(j)} - \bar{\hat{x}}_k^{-})(\hat{x}_k^{-(j)} - \bar{\hat{x}}_k^{-})^T \tag{S10}$$

Field Code Changed

where $\hat{x}_k^{-(j)}$ is the propagated state vector at time *k* for the *j*th ensemble member, and $\bar{\hat{x}}_k^{-}$ is the mean of $\hat{x}_k^{-(j)}$ across all ensemble members;

Field Code Changed

Field Code Changed

Field Code Changed

4) Following the calculation of *K*, each ensemble member of states (only the first and second VIC SM layers from the top) is individually updated as:

$$\hat{x}_k^{+(j)} = \hat{x}_k^{-(j)} + K_k \cdot (\tilde{y}_k + v_k^{(j)} - \hat{y}_k^{-(j)}) \tag{S11}$$

Field Code Changed

where $\hat{y}_k^{-(j)}$ is the simulated measurement at time *k* for the *j*th ensemble member, i.e., $\hat{y}_k^{-(j)} = H\,\hat{x}_k^{-(j)}$; $v_k^{(j)}$ is random noise added to represent measurement error whose error statistic is consistent with *R* in Eq. (S9).

Field Code Changed

Field Code Changed

Field Code Changed

S3. The sensitivity of the SMART rainfall correction performance to the γ parameter

The unit-less γ parameter in Eq. (1) in the main manuscript was tuned such that the API model (approximately) optimally captured the SM dynamic observed by SMAP. We further carried out a sensitivity analysis of the rainfall correction performance to γ. Specifically, we varied γ to see its impact on the correlation coefficient improvement and percent RMSE reduction (PER). Figures S1 and S2 show the domain-median of both evaluation metrics, respectively, after correction at different γ values (in the manuscript, $\gamma = 0.98$ was used). We see that around our chosen value $\gamma = 0.98$, the sensitivity of rainfall correction performance to γ is relatively small, and $\gamma = 0.98$ results in optimal PER when evaluating SMART results at 1-day and 3-day accumulation periods (although performance is even slightly better at $\gamma = 0.99$ for the other measures shown). However, we also see that the correction performance is significantly degraded if γ is far from our chosen value (i.e., if $\gamma < 0.95$). These results should generally confirm that our selected γ value in the manuscript is reasonable and roughly optimal.

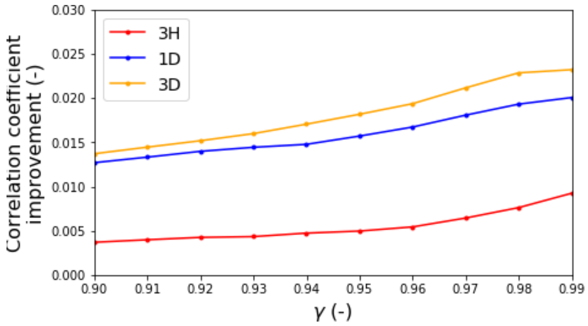

Figure S1. Domain-median correlation coefficient improvement of IMERG rainfall after SMART correction (with respect to the NLDAS-2 reference) using different γ values. Improvement is evaluated for 3-hour (3H), 1-day (1D) and 3-day (3D) accumulation intervals.

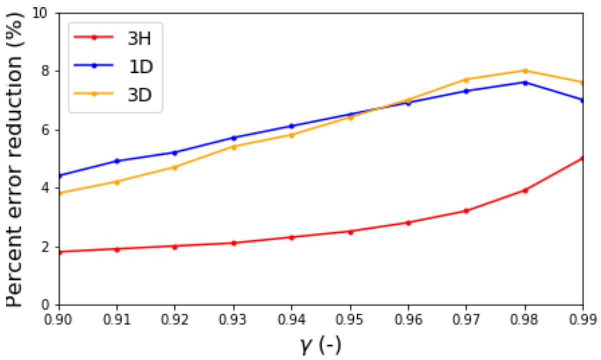

Figure S2. Same as Fig. 1, but for RMSE reduction (PER) evaluations.

S4. The impact of the λ parameter in the SMART rainfall correction scheme

In the SMART rainfall correction scheme, λ is a unit-less scaling factor that linearly relates the API state increment to rainfall correction amount. It can either be calibrated or set to a prescribed constant. We experimented with two strategies of determining λ in this study: 1) calibrating a temporally constant λ at each SMAP pixel separately to optimize the rainfall correlation with respect to the NLDAS-2 benchmark rainfall, and 2) setting λ to a spatial constant of 0.1, which is applicable for any region that may not have a good rain gauge coverage.

The rainfall correction results from the two strategies are shown in Fig. ~~S1~~S3, in which ~~Column~~column 1 shows the improvement of correlation coefficient r after SMART correction with λ tuned at each pixel to maximize r (with respect to the NLDAS-2 benchmark), and ~~Column~~column 2 shows results obtained using a domain-constant value of $\lambda = 0.1$. Simply setting $\lambda = 0.1$ results in slightly smaller correlation improvement compared to the optimal λ case for all examined temporal accumulation periods (3-hour, 1-day and 3-day), especially for locations in the eastern and western ends of the domain. In general, these reductions are small, and since constant-λ is a more generally applicable case, we ~~decided to use~~selected the $\lambda = 0.1$ ~~strategies~~strategy for all the SMART results presented in the main manuscript.

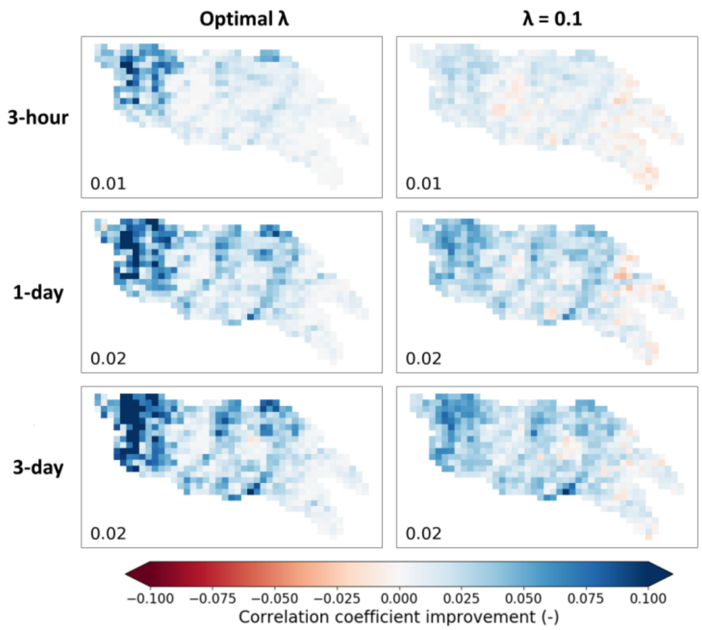

Figure ~~S1~~S3. Maps of correlation coefficient improvement after SMART EnKS rainfall correction. The left column shows the results with λ tuned at each pixel to optimize the correlation coefficient of corrected rainfall relative to the NLDAS-2 benchmark, and the right column shows the results with domain-constant λ = 0.1 ~~[-]~~ (this column is identical to the left column in Fig. 3 in the main manuscript). Each row shows results based on different temporal accumulation ~~period~~periods: 3-hourly, 1-day and 3-day aggregation, respectively. The number on the lower left corner of each subplot shows the domain-median correlation improvement.

~~S3~~S5. Investigation of cross-correlation of errors in the dual system

~~S3~~S5.1. Background and methods

It is well known that correlated errors in different parts of a Kalman filter result in sub-optimal filter outputs. Therefore, in the original paper detailing the dual state/rainfall correction system, Crow and Ryu (2009) advised that the corrected rainfall (informed by the SM measurements) should not be fed back into the state EnKF correction scheme into which the same SM measurements are assimilated. Instead, corrected rainfall and states should be combined via an offline model simulation (see Fig. 1 and Sect. 2.4.3 in the main manuscript). Later studies that applied the dual correction system all followed this general guideline (e.g., Chen et al., 2014; Alvarez-Garreton et al., 2016). However, although this guideline ~~helps avoid~~avoids first-order error correlation in the system, it does not ~~completely~~ eliminate the possibility of error cross-correlation. Specifically, the corrected rainfall and the updated states are informed by the same SM measurement, thus they potentially inherit the same error from the SM ~~measurement. When fusing the two schemes together, such inherited error could potentially be amplified, degrading streamflow performance or cause a probabilistic estimate (based on an implicit assumption of independent errors) to be biased or have inaccurate uncertainty spread. In other words, it is possible that the current system still suffers from some second-order issue of overusing the information of SM measurements. Massari et al. (2018) intentionally avoided combining the state update scheme and the rainfall correction scheme in their study due to this legitimate concern.~~measurements. See Sect. 2.4.3 in the main manuscript for more details.

To further investigate this issue, we designed a set of synthetic experiments and applied in an arbitrary small domain within the Arkansas-Red (a box around the Little Arkansas subbasin, see Table 1 and Fig. 2 in the main manuscript for its location). Synthetic measurements, instead of the real SMAP measurements, were generated and assimilated into the dual correction system so that we have complete control over all the error statistics and correlation, which is impossible in a real-data case. Specifically, a single perturbed VIC realization (with perturbed forcing and states) was treated as the synthetic “truth”. Synthetic measurement can then be generated at daily interval by degrading the true surface-layer SM by adding random measurement errors. Precipitation perturbation was assumed to be temporally auto-correlated (first-order autoregressive noise with parameter ϕ = 0.9), and all the other error assumptions and dual correction setup were consistent with those described in Sect. 2.4 in the main manuscript.

We generated two sets of synthetic measurements based on the same truth with the same measurement error statistics but mutually independent realizations of errors. Then, two scenarios of dual correction were designed and carried out (see Fig. ~~S2~~S4 for illustration):

Scenario 1: ~~the same set~~a single time series of synthetic SM ~~measurement~~measurements were assimilated into both the state update and the rainfall correction schemes. This scenario mimics the issue in the real-data dual system with error cross-correlation in the two schemes and potentially degraded streamflow;

Scenario 2: two ~~sets~~different time series of~~ synthetic~~ SM measurements (with mutually independent errors) were assimilated into the two schemes separately. This scenario completely avoids the issue of error cross-correlation.

The final runoff performance from the dual correction system were evaluated toward the truth, and the runoff performance from the two scenarios was compared. Differences in the performance of the two scenarios would indicate degradation caused by error cross-correlation~~.~~ present in Scenario 1. For these synthetic experiments, runoff was evaluated locally at each grid cell without routing, since we know the true condition locally.

~~S3~~S5.2. Results

Deterministic and probabilistic results from the two scenarios were compared in Fig. ~~S3~~S5 and Fig. ~~S4~~S6. Clearly, runoff results show only very little difference between the two scenarios in terms of both PER and NENSK (see Sect. 2.5 in the main manuscript for details of the two metrics). This is true for both the total runoff and the fast- and slow-response runoff components separately. This suggests that the streamflow performance is not noticeably degraded by assimilating the same SM retrievals to both the state update and rainfall correction schemes. Although ~~the~~ cross-correlated error theoretically exists in the system, ~~they are~~it is not ~~big~~persistent enough to cause problematic streamflow results. In other words, we are not significantly over-using the information contained in SM retrievals in the system. This is true both from a deterministic sense and in terms of probabilistic representation. We also experimented the case where the synthetic measurements were assumed to have temporally auto-correlated errors instead of white errors, which in theory creates ~~bigger~~an enhanced risk of degradation in the subsequent streamflow, but drew similar conclusions as above (results not shown).

The synthetic results in this section ~~validates~~verifies that we can safely assimilate ~~the~~ a single time series of SMAP retrievals into both ~~schemes~~parts of the dual correction system without significantly degrading the final streamflow ~~performance~~estimates.

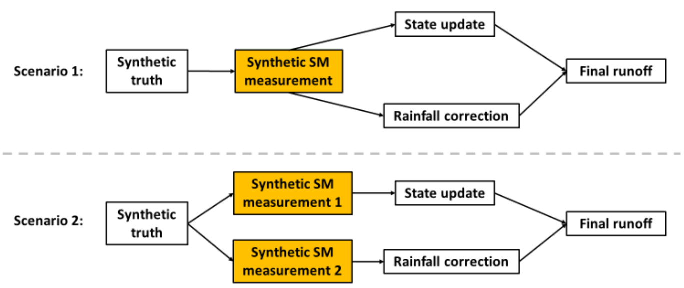

Figure ~~S2~~S4. Illustration of the synthetic experiments for investigating error cross-correlation.

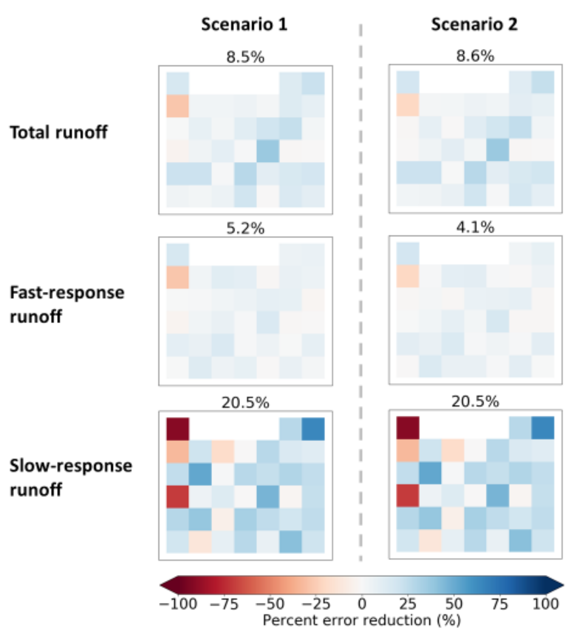

Figure ~~S3~~S5. ~~Percent RMSE reduction (~~PER~~)~~ of synthetic daily runoff results from the error cross-correlation experiment. Blue color indicates runoff improvement after dual correction while red color indicates degraded runoff. The two columns show the results from the two assimilation scenarios described in Sect. ~~S3~~S5. The three rows show results of total runoff, fast-response runoff and slow-response runoff, respectively. The number on top of each subplot indicates the domain-median PER.

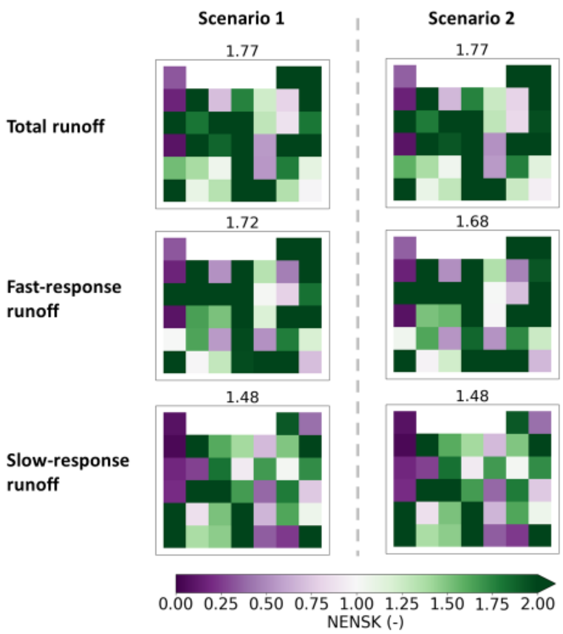

Figure ~~S4~~S6. Same as Fig. ~~S3~~S5 but for NENSK. Lighter color (either green or purple) indicates closer-to-one (thus better) NENSK.

S6. Sensitivity analysis of SMART rainfall correction performance to rain/no rain threshold

We have added a sensitivity analysis of SMART rainfall correction performance to rain/no rain threshold. Specifically, we altered the threshold of classifying IMERGE rain/no rain (this threshold was essentially set to zero in the manuscript and SMART only corrected time steps during which non-zero rainfall occurs), and observed its impact on the rainfall correction results (i.e., categorical metrics at different rainfall scales as well as correlation improvement and PER).

Figures S7 to S9 show the SMART correction results with different rain/no rain thresholds. For categorical metrics (Fig. S7), having a rain/no rain accumulation threshold of 1 mm/3 hours or 2 mm/3 hours mitigates the issue of worsened POD at small rainfall events comparing to zero threshold, but also removes the (although small) FAR improvement. For mid-ranged rainfall events, a positive threshold mitigates the issue of worsened FAR as in the zero-threshold case, but POD improvement becomes smaller. For larger rainfall events, POD improvement and TS improvement become slightly smaller (i.e., closer to zero) when using a positive rain/no rain threshold (note that the small positive rain/no rain threshold value can be considered as a “larger” rainfall event percentile wise at some pixels with overall low precipitation, therefore affecting the categorical metrics toward the right side on the categorical metrics plots).

In addition to the categorical metrics, setting the rain/no rain threshold to either 1 mm/3 hours or 2 mm/3 hours slightly lowers values of correlation coefficient improvement and PER versus the baseline case of applying a rain/no rain threshold of zero accumulation (Figures S8 and S9).

In summary, there is no obvious optimized (non-zero) value for the rain/no rain threshold since there is a trade-off between POD and FAR performance. Although the overall TS at smaller rainfall events improves with a non-zero threshold, the correction for larger events, which SMART is most suitable for, slightly worsens. Therefore, a positive rain/no rain threshold does not benefit correlation coefficient and PER (which are sensitive to both POD and FAR performance). Based on this analysis, we selected a zero rain/no rain threshold for all SMART correction results presented in the main manuscript.

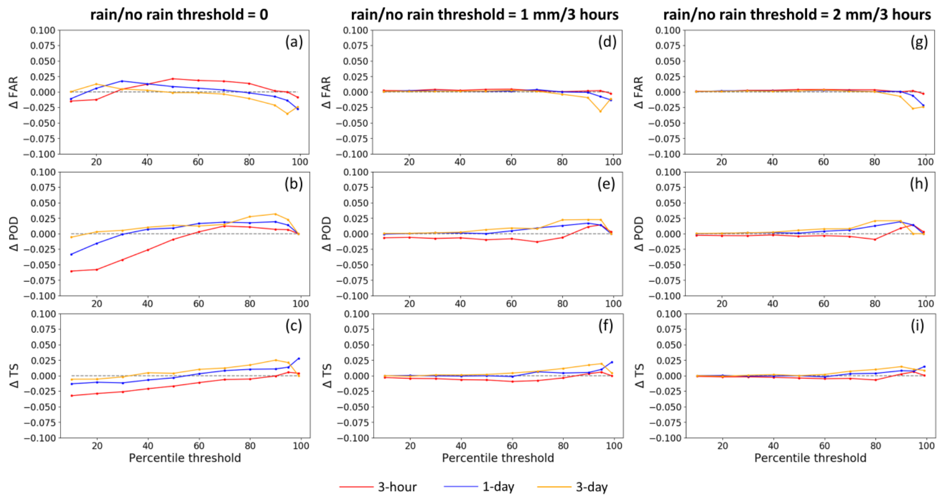

Figure S7: Change in categorical metrics (FAR, POD and TS) before and after SMART correction for 3-hourly, 1-day and 3-day accumulation periods. The left column (panels a, b and c) is the same as in Fig. 4 (right column) in the main text with SMART only correcting IMERG rainfall events with non-zero accumulation. The middle and right columns show the same metrics with SMART only correcting IMERG rainfall for events where accumulation rates exceed thresholds of 1 mm/3 hours and 2 mm/3 hours, respectively.

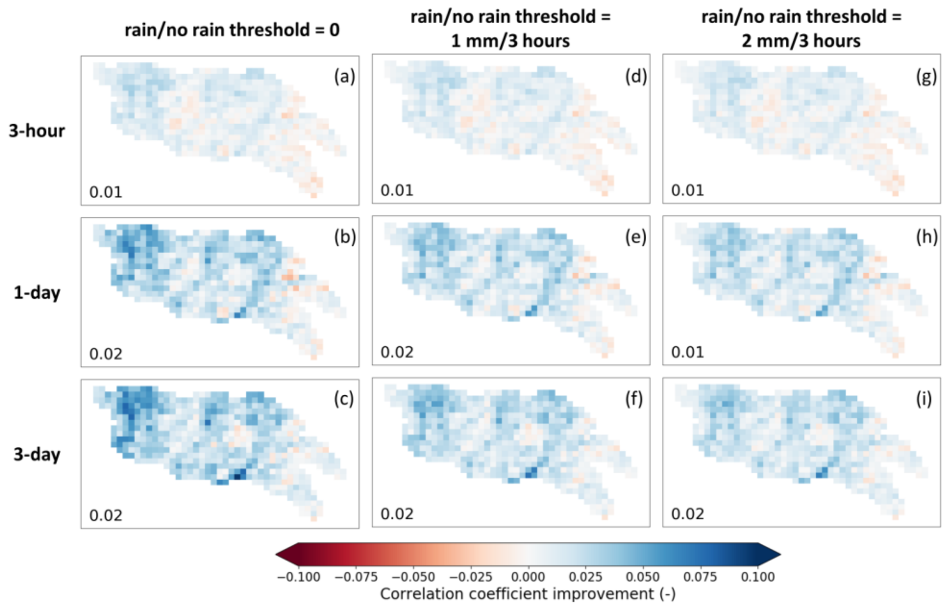

Figure S8: Correlation coefficient (with respect to the NLDAS-2 reference precipitation) improvement before and after SMART correlation for 3-hourly, 1-day and 3-day accumulation periods. As in Fig. 7, the left column (panels a, b and c) is the same as in Fig. 4 (right column) in the main text with SMART only correcting IMERG rainfall events with non-zero accumulation. The middle and right columns show the same metrics with SMART only correcting IMERG rainfall for events where accumulation rates exceed thresholds of 1 mm/3 hours and 2 mm/3 hours, respectively.

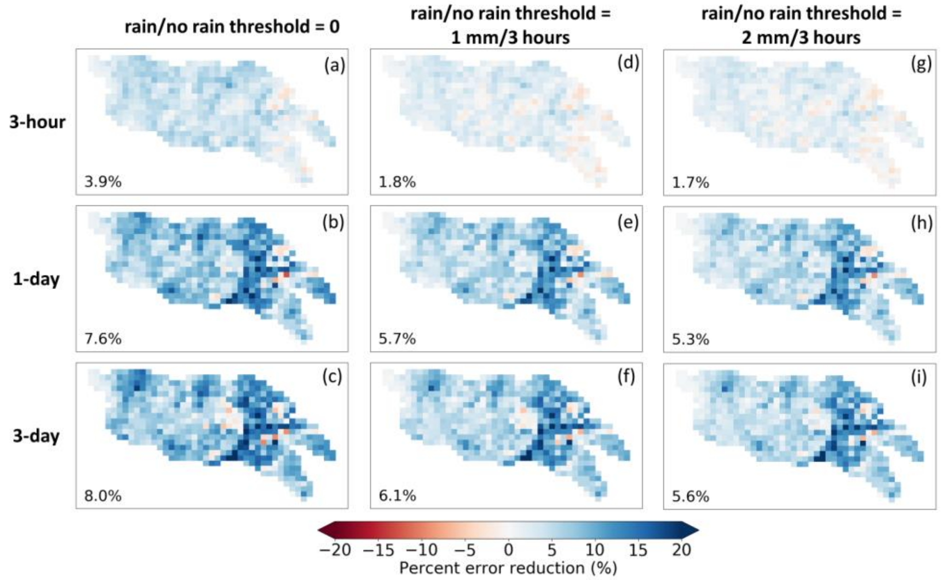

Figure S9: Same as Fig 8, but for percent RMSE reduction (PER; with respect to the NLDAS-2 reference precipitation). The left column (panels a, b and c) is the same as in Fig. 5 (left column) in the main text.

References:

Alvarez-Garreton, C., Ryu, D., Western, A. W., Crow, W. T., Su, C.-H., and Robertson, D. R.: Dual assimilation of satellite soil moisture to improve streamflow prediction in data-scarce catchments, Water Resour. Res., 52(7), 5357-5375, doi:10.1002/2015WR018429, 2016.

Chen F., Crow, W. T., and Holmes, T. R. H.: Improving long-term, retrospective precipitation datasets using satellite-based surface soil moisture retrievals and the Soil Moisture Analysis Rainfall Tool, J. Appl. Remote Sens., 6(1), 063604, doi:10.1117/1.JRS.6.063604, 2012.

Chen, F., Crow, W. T., and Ryu, D.: Dual forcing and state correction via soil moisture assimilation for improved rainfall–runoff modeling, J. Hydrometeorol., 15(5), 1832–1848, doi:10.1175/JHM-D-14-0002.1, 2014.

Crow, W. T., and Ryu, D.: A new data assimilation approach for improving hydrologic prediction using remotely-sensed soil moisture retrievals, Hydrol. Earth Syst. Sci., 12(1-16), doi:10.5194/hess-13-1-2009, 2009.

Crow W. T., Huffman, G. J., Bindlish, R., and Jackson, T. J., Improving satellite-based rainfall accumulation estimates using spaceborne surface soil moisture retrievals, J. Hydrometeorol., 10, 199-212, doi:10.1175/2008JHM986.1, 2009.

Crow, W. T., van den Berg, M. J., Huffman, G. J., and Pellarin, T.: Correcting rainfall using satellite-based surface soil moisture retrievals: The Soil Moisture Analysis Rainfall Tool (SMART), Water Resour. Res., 47, W08521, doi:10.1029/ 2011WR010576, 2011.

~~Massari, C., Camici, S., Ciabatta, L., and Brocca, L.: Exploiting satellite-based surface soil moisture for flood forecasting in the Mediterranean area: State update versus rainfall correction, Remote Sens., 10, 292, doi:10.3390/rs10020292, 2018.~~

Mao Y., Crow, W. T., and Nijssen, B.: A framework for diagnosing factors degrading the streamflow performance of a soil moisture data assimilation system, J. Hydrometeorol., 20(1), 79-97, doi:10.1175/JHM-D-18-0115.1, 2019.